



Titre: Reader Design for Chipless Millimeter-Wave Identification
Title: (MMID)TAG

Auteur: Wencui Zhu
Author:

Date: 2017

Type: Mémoire ou thèse / Dissertation or Thesis

Référence: Zhu, W. (2017). Reader Design for Chipless Millimeter-Wave Identification (MMID)TAG [Mémoire de maîtrise, École Polytechnique de Montréal]. PolyPublie.
Citation: <https://publications.polymtl.ca/2693/>

 **Document en libre accès dans PolyPublie**
Open Access document in PolyPublie

URL de PolyPublie: <https://publications.polymtl.ca/2693/>
PolyPublie URL:

Directeurs de recherche: Ke Wu
Advisors:

Programme: génie électrique
Program:

UNIVERSITÉ DE MONTRÉAL

READER DESIGN FOR CHIPLESS MILLIMETER-WAVE IDENTIFICATION (MMID) TAG

WENCUI ZHU

DÉPARTEMENT DE GÉNIE ÉLECTRIQUE

ÉCOLE POLYTECHNIQUE DE MONTRÉAL

MÉMOIRE PRÉSENTÉ EN VUE DE L'OBTENTION
DU DIPLÔME DE MATÎRISE ÈS SCIENCES APPLIQUÉES

(GÉNIE ÉLECTRIQUE)

JANVIER 2017

© Wencui Zhu, 2017.

UNIVERSITÉ DE MONTRÉAL

ÉCOLE POLYTECHNIQUE DE MONTRÉAL

Ce mémoire intitulé :

READER DESIGN FOR CHIPLESS MILLIMETER-WAVE IDENTIFICATION (MMID) TAG

présenté par : ZHU Wencui

en vue de l'obtention du diplôme de : Matrise ès sciences appliquées

a été dûment accepté par le jury d'examen constitué de :

Mme SANSO Brunilde, Ph. D, présidente

M. WU Ke, Ph. D, membre et directeur de recherche

M. TATU Serioja Ovidiu, Ph. D, membre

DEDICATION

To my family

ACKNOWLEDGEMENTS

First of all, I would like to give my deep thanks to my supervisor Professor Ke Wu, for his guidance, support and understanding throughout my studies at Polytechnique Montreal. His passion about research, his attitude towards every detail things in daily work have really inspired me and will affect me in my future life. I also would like to thank Doc Tarek Djerafi. My system cannot be finished without his consistent help in the last two years.

I would also like to thank all the personnel in Poly-Grames Research Center, in particular the technician group members including Mr. Jules Gauthier, Mr. Steve Dube, Mr. Traian Antonescu and Mr. Maxime Thibault for their great skills in circuit fabrication and measurement. My gratitude is extended to Mrs. Nathalie Lévesque as well as Mrs. Rachel Lortie for their administrative work and to Mr. Jean Seasteien Dearie for his IT support.

I am indebted to all my colleagues. I want to especially thank Kuangda Wang, Yangping Zhao and Jiming Li for their support in both studies and personal life. For students work in M6002 including Ruizhi Liu, Zoe and Ahmit, it is always nice to work with you all.

I would like thank all the jury members for their time and efforts in revising my thesis and giving me such precious suggestions

Last but not least, I would like thank my whole family including me parents and my twin brother. Family is always the first place for me. We support each other, love each other and being best friends with each other all the time.

RÉSUMÉ

L'identification par radiofréquence (RFID) est une technologie d'identification qui a de nombreuses applications utiles telles que le suivi des marchandises et les contrôles d'accès. RFID est une technique de transmission et réception à courte distance « sans-contact » pour envoyer des données ID à un lecteur à partir d'un objet marqué. Un système RFID se compose d'une étiquette de support de données, un lecteur, un middleware et une application d'entreprise. Tout d'abord, le signal transmis est généré par le lecteur, après une certaine distance de transmission dans l'espace libre, l'étiquette reçoit le signal détecté et après le traitement de signal ou codage du signal sur l'étiquette, le signal codé est renvoyé au lecteur. La réception et le traitement du signal seront finalement faits au récepteur. Cependant, la technologie RFID est entravée en raison de son prix élevé. Les étiquettes RFID sans puce résolvent le problème de coût et ont le potentiel de pénétrer aux marchés en grand public pour l'étiquetage de l'article à faible coût. Pour les étiquettes sans puce il n'y a pas de traitement de signal. Le traitement du signal se fait uniquement au niveau du lecteur. Ainsi, un lecteur qui est utilisé pour communiquer avec l'étiquette est également important dans un système de communication. Le domaine de fréquence ou la signature spectrale en fonction des étiquettes sans puce est un type d'étiquette sans puce. D'autre part, l'émetteur et le récepteur se composent d'un lecteur. Basé sur le principe de fonctionnement des étiquettes sans puce dans le domaine de fréquence, un lecteur comprend un émetteur et un récepteur utilisés pour communiquer avec une étiquette de fréquence et est présenté dans cette thèse.

Tout d'abord, le principe de fonctionnement détaillé du système MMID sans puce, dans le domaine fréquentiel est introduit. D'autre part, sur la base du principe de fonctionnement, les spécifications de la conception du lecteur sont proposées. Plusieurs topologies différentes de la conception du lecteur seront comparées et la meilleure topologie sera sélectionnée pour la conception du lecteur.

En second lieu, sur la base des spécifications du système de lecture et de la topologie sélectionnée, les résultats de simulation de la structure sélectionnée de lecteur sont présentés. Après les simulations, la conception de chaque composant est montrée. Dans cette conception de système des circuits, tous les circuits passifs sont conçus et simulés dans HFSS et mesurés sur VNA. Tous les circuits actifs sont des puces commerciales de différentes compagnies. Les résultats des simulations et mesures de chaque circuit passif sont affichés.

Enfin, l'ensemble des circuits, y compris les circuits passifs conçus et circuits actifs sont intégrés dans un système de carte pour combiner un système de lecteur. Le système de lecteur se compose d'un émetteur et d'un récepteur. Le système d'émetteur-récepteur entier est finalement testé.

ABSTRACT

Radiofrequency identification (RFID) technology is an identification technology that has many useful applications such as tracking goods and access controls. RFID is a touchless, short distance transmission and reception technique for ID data that is sent from a labeled object to a reader. A data-carrying tag, a reader, middleware and an enterprise application would make up a RFID system. Firstly, the transmitted signal is generated by the reader, the tag receiver, after a certain distance of transmission in free space, a detected signal and after processing signal or encoding signal on the tag, the encoded signal is then sent back to the reader. Signal receiving and processing part will be finally processed in the receiver.

However, the RFID technology is hindered because of its high price tag. Chipless RFID tags solve the cost issues and have the potential to penetrate into mass markets for low-cost item tagging. For chipless tags, there is no signal processing in tags, the signal processing is done only in the reader. So a reader, which is used to communicate with the tag, is also important in a communication system. Frequency domain or spectral signature-based chipless tags are some kinds of chipless tag. On the other hand, transmitter and receiver are the core parts of a reader, based on the working principle of frequency domain chipless tags, a reader that includes a transmitter and a receiver used to communicate with frequency tag is presented in this dissertation.

First of all, the detailed working principle of a chipless MMID system in the frequency domain is introduced. Based on the working principle, the specifications of the reader design are proposed. Several different topologies of the reader design will be compared and the best topology will be selected for our reader design.

Secondly, based on the specifications of the reader system and the selected topology, the simulation results of the selected structure of the reader are presented. After the simulations, the design of each component is shown. In this system design, all the passive circuits are designed and simulated in HFSS and tested on VNA. All the active circuits are commercial chips from different companies. Simulation and measurement results for each passive circuit are given.

Finally, the whole circuits including designed passive circuits and active circuits are integrated into a system board to create a reader system. There are two system boards finally fabricated, one transmitter board and one completed reader board. The transmitter board is tested firstly. Upon achieving good results of the transmitter board, the whole transceiver board is tested finally.

TABLE OF CONTENTS

DEDICATION.....	iii
ACKNOWLEDGEMENTS.....	iv
RÉSUMÉ.....	v
ABSTRACT.....	vii
TABLE OF CONTENTS.....	viii
LIST OF TABLES.....	x
List OF FIGURES.....	xi
LIST OF SYMBOLS AND ABBREVIATIONS.....	xv
CHAPTER 1 INTRODUCTION.....	1
CHAPTER 2 DESIGN CONSIDERATIONS AND SYSTEM CONCEPT.....	4
2.1 Operating principle of chipless frequency domain based system	4
2.2 Typical circuits and system parameters in reader design	5
2.2.1 Antenna	5
2.2.2 Filters.....	6
2.2.3 Coupler and power divider	7
2.2.4 Mixer	8
2.2.5 Amplifier	9
2.2.6 VCO (Voltage controlled oscillator).....	9
2.2.7 Noise figure of receiver.....	11
2.2.8 Sensitivity.....	12
2.2.9 1 dB compression point.....	13
2.2.10 Third-order intercept point	13
2.3 Three methods to generate FMCW signal.....	16

2.4	Different reader topologies comparison	18
CHAPTER 3 SYSTEM SIMULATION AND CIRCUITS DESIGN.....		21
3.1	System simulation	21
3.2	Circuits design of reader system	26
3.2.1	AD 9914 (DDS)	26
3.2.2	HMC765 (PLL).....	27
3.2.3	Microstrip line and ground coplanar waveguide (GCPW).....	28
3.2.4	Stepped-impedance low-pass filter	29
3.2.5	HMC573 (Multiplier).....	31
3.2.6	Band-pass filter design	32
3.2.7	Low-pass filter after AD9914	37
3.2.8	17.5-18 GHz Wilkinson power divider design.....	38
3.2.9	Two SIW filters design	41
3.2.10	HMC579 (Multiplier).....	45
3.2.11	LC bandpass filter design.....	46
3.2.12	VGA (variable gain amplifier) module design.....	47
CHAPTER 4 SYSTEM MEASUREMENT.....		51
4.1	Transmitter Measurement	51
4.2	Measurements of the transceiver system.....	53
CONCLUSION AND FUTURE WORK.....		57
BIBLIOGRAPHY		59

LIST OF TABLES

Table 3.1. Specifications of our proposed reader design.	21
Table 3.2 Components and their realizations of transmitter	24
Table 3.3 Components and their realizations of receiver	24
Table 3.4. System simulation results of transmitter.	25
Table 3.5. System simulation results of receiver.	25
Table 3.6 Dimensions of the six-order stepped-impedance low-pass filter	30
Table 3.7 Dimensions of the six-order stepped-impedance low-pass filter	33
Table 3.8. Dimensions of the designed 17.5-18 GHz SIW filter.	43
Table 3.9. Dimensions of the designed 36-36 GHz SIW filter.	44
Table. 4.1. Active circuits and their DC supplies of reader.	53

LIST OF FIGURES

Figure 1.1. A RFID system [4].....	1
Figure 2.1. Structure and operation of a typical chipless tag encoded in the frequency domain [3].	4
Figure 2.2. Transmitted signal in the time domain.	5
Figure 2.3. Typical encoded signal of frequency domain based chipless tag [3].	5
Figure 2.4. Various types of antennas in communication system [10].	6
Figure 2.5. Four types of filters: (a) low-pass, (b) high-pass, (c) band-pass, (d) band-stop [10]. ...	6
Figure 2.6. Power division and combining [12].....	7
Figure 2.7. Widely used circuit symbols of coupler [3].....	8
Figure 2.8. Frequency conversion with mixer. (a) Up-converter. (b) Down-converter [12].	8
Figure 2.9. Amplifier with power gain [10].	9
Figure 2.10. Typical schematic for a varactor based VCO [3].	10
Figure 2.11. Method to generate millimeter-wave signals [3].	10
Figure 2.12. Two ports network.	11
Figure 2.13. Typical cascaded circuit [12].	12
Figure 2.14. 1dB point.....	13
Figure 2.15. Signals generated from two RF signals [12].....	14
Figure 2.16. Intermodulation products [10].	15
Figure 2.17. Relation between 1 dB compression point and IP3 point.	15
Figure 2.18. A typical PLL.....	16
Figure 2.19. First method to generate wideband signal with DDS and PLL.	16
Figure 2.20. PLL and DDS mix up to generate wideband signal.....	17
Figure 2.21. Generation of a wideband frequency signal using a VCO [3].	17

Figure 2.22. First topology of the transmitter.	18
Figure 2.23. Second topology of the transmitter.	18
Figure 2.24. Output signal of sub-harmonic mixer in second topology.....	19
Figure 2.25. The third topology of transmitter.....	20
Figure 3.1. Measurement set up for chipless MMID tag [17].....	22
Figure 3.3. Proposed reader structures for chipless MMID tag.	23
Figure 3.4. System simulation in ADS.....	25
Figure 3.5. Signal source of transmitter.	26
Figure 3.6. Internal structure of AD9914.....	27
Figure 3.7. Evaluation boards of HMC765 and DDS9914.	27
Figure 3.8. Phase noise of output signal generated by HMC765.....	28
Figure 3.9. Microstrip line [12].....	28
Figure 3.10. GCPW transmission line.....	29
Figure 3.11. Geometry of the six-order stepped-impedance low-pass filter.....	30
Figure 3.12. Fabricated stepped impedance low pass filter.	30
Figure 3.13. simulation and test results of the stepped-impedance low-pass filter.....	31
Figure 3.14. Test result of HMC573.	32
Figure 3.15. The schematics of the forming process of a wide-band band-pass filter[18].	32
Figure 3.16. Designed six-order stepped impedance low pass filter.....	33
Figure 3.17. Simulation results of the stepped impedance low pass filter.	34
Figure 3.18. Geometry of an SIW [19].	35
Figure 3.19. Two transitions from planar circuits to SIW (a) microstrip line, (b) conductor backed CPW line [25].....	35
Figure 3.20. Structure of SIW transmission line.	36
Figure 3.21. Simulated results of an SIW transmission line.	36

Figure 3.22. Simulated and measured results of the wideband band-pass filter.	37
Figure 3.23. Fabricated wideband band-pass filter.	37
Figure 3.24. Measured result of the low-pass filter from Mini-circuits.	38
Figure 3.25. The structure of Wilkinson power divider [12].	39
Figure 3.26. Proposed structure of Wilkinson power divider in [29].	39
Figure 3.27. Fabricated 17.5-18 GHz Wilkinson power divider.	40
Figure 3.28. Simulated results of our Wilkinson power divider.	40
Figure 3.29. Measured results of our Wilkinson power divider.	41
Figure 3.30. Different types of SIW filters. (a) Filter with inductive-post, (b) Filter with iris windows, (c) Filter with circular cavities, (d) Filter with rectangular cavities and cross-coupling. [19].	42
Figure 3.31. Layout of the designed 17.5-18 GHz SIW filter.	42
Figure 3.32. Measured and simulated results of the 17.5-18 GHz SIW filter.	43
Figure 3.33. Fabricated 17.5-18 GHz SIW filter.	43
Figure 3.34. Layout of the designed 36-36 GHz SIW filter.	44
Figure 3.35. Simulated and measured results of our 35-36 GHz SIW filter.	45
Figure 3.36. Fabricated 35-36 GHz four SIW cavities filter.	45
Figure 3.37. Wire-bonding technique under our microscope.	46
Figure 3.38. Schematic diagram of the LC bandpass filter.	47
Figure 3.39. Measured result of the LC bandapss filter.	47
Figure 3.40. Circuits structure of the LC bandpass filter and the VGA circuits.	48
Figure 3.41. Circuit board contains LC filter and VGA circuits.	48
Figure 3.42. Output power at 1.5 MHz.	49
Figure 3.43. Output power at 3 MHz.	49
Figure 3.44. Output signal at 4MHz.	50

Figure 4.1. Fabricated transmitter of our reader system.	51
Figure 4.2. Phase noise of one tone signal.	52
Figure 4.3. Output signal of our transmitter.	52
Figure 4.4. Fabricated power supply board.	53
Figure 4.5. Fabricated reader system with a metallic housing.	54
Figure 4.6. Measured results of the transceiver (a) transmitted signal, (b) output at 4 MHz.	55

LIST OF SYMBOLS AND ABBREVIATIONS

ADS	Advanced Design System
CPW	Coplanar waveguide
DDS	Direct Digital Synthesizer
EMC	Electromagnetic Compatibility
EMI	Electromagnetic Interference
FCC	Federal Communications Commission
GCPW	Grounded Coplanar waveguide
HFSS	High frequency structure simulator
IF	Intermediate Frequency
LNA	Low noise amplifier
LO	Local oscillator
MMID	Millimeter-wave Identification
NF	Noise Figure
PA	Power Amplifier
PCB	Printed circuit board
RF	Radio frequency
RFID	Radio Frequency Identification
PCB	Printed Circuit Board
PLL	Phase-Locked Loop
SIW	Substrate Integrated (Rectangular) Waveguide
SMA	Subminiature Version A
SNR	Signal-to-Noise Ratio
UHF	Ultra-High-Frequency

VGA	Variable Gain Amplifier
VHF	Very-High-Frequency
VNA	Vector Network Analyzer
VSWR	Voltage Standing Wave Ratio

CHAPTER 1 INTRODUCTION

Radiofrequency identification (RFID) is a contactless wireless data-capturing technology that utilizes radiofrequency (RF) waves for data transmission between reader and tag [1]. In recent years, applications of RFID are widespread. Inductive RFID systems at low-frequency (LF) and high-frequency (HF) bands are widely adopted. Ultra high-frequency (UHF) band has also been utilized for RFID [2]. These different frequency ranges of RFID system are widely used in variety of applications such as access management, tracking of goods, toll collection or contactless payment and machine readable travel documents. Thanks to large information-carrying capacity, flexibility in operation and versatility in application, RFID technology has the potential to replace barcodes in the future [3].

A RFID system mainly has two parts, namely reader and tag. The reader sends an interrogating signal to the tag, and the tag then receives the signal and return a signal after encoding process in the tag. The reader processes the returned signal from the tag.

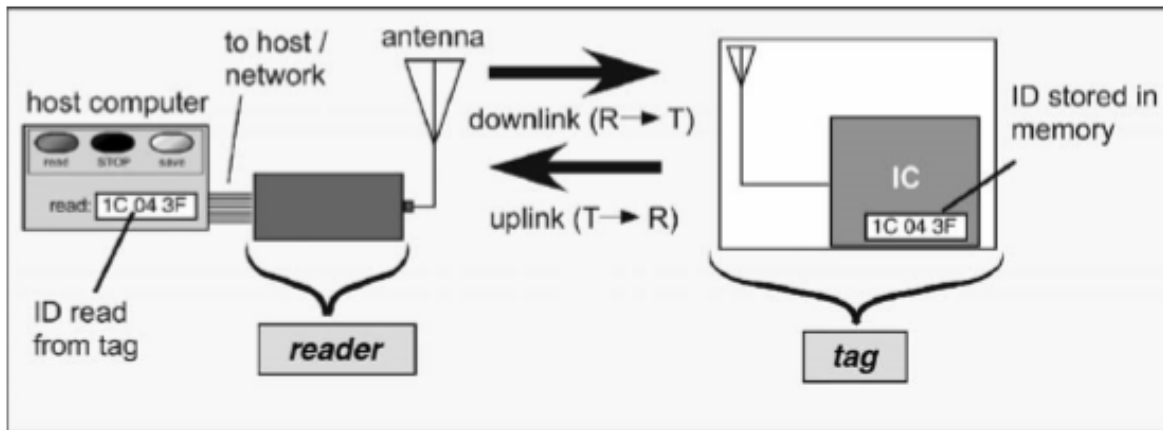


Figure 1.1. A RFID system [4].

Generally, there are three kinds of tags: passive tags, active tags and semi-passive tags. They are based on whether have on-board power supply in tags or not [4]. These three kinds of tags have their own advantages and disadvantages and are widely used in different fields. A tag in which there is no on-board power supply is called passive tag. For a RFID tag design, cost of the tag is an important issue to consider. Hence lots of effort have been put in developing RFID system which should cost in the design consideration. The cost of an entire RFID system is dependent on the cost of tag which depends on the cost of its own IC [5]. In order to reduce the price of tags, chipless

RFID tags have been developed. Chipless tag is one kind of fully passive tag because there is no integrated circuit (IC) on tag. The chipless tag has well-spelled advantages over conventional passive HF and UHF tags such as low cost, fully printable and more robust. Generally there are two kinds of chipless tag: 1) time domain TDR based chipless RFID tags and 2) frequency domain (spectral signature) based chipless RFID tags. In this research, chipless MMID tag encodes information in the frequency domain. The detailed operation principle of chipless tag in the frequency domain would be introduced in Chapter 2.

On the other hand, millimeter-wave identification (MMID) enables the working frequency at the millimeter wave frequency band. There are several advantages when working frequency is at millimeter frequency range [6] [5] [1] [7]. Over the millimeter wave range, the antenna becomes smaller. Smaller antenna makes tag more compact and reader modules as well. Secondly over the millimeter wave frequency range, a reader device with a small directive antenna would provide a possibility of selecting a transponder by pointing toward it. This is not possible in today's UHF RFID systems because directive antennas are too large. A directive reader antenna would help in locating transponders in high-density sensor networks or other places where transponders are densely located, e.g., in item level tagging [6]. Thirdly, antenna arrays can be used to achieve narrow beam reader antennas, which enable efficient transponder localization. Finally, at millimeter waves frequencies, high data-rate communications with even gigabit data rates can be implemented.

The reader in a RFID/MMID communication system plays the role of sending, receiving and analyzing the signal. It is also crucial to design a reliable reader for chipless tag use. The reader is also called "interrogator". In chipless RFID technology, the architecture of a reader design needs to be different based on different types of tag design [3]. A research group from Australia proposed two reader structures for identifying chipless tags [3]. The proposed two reader structures include two parts, digital part and RF part. The information in the frequency domain is finally decoded after signal processing in the digital part. In their research work, the working frequency of the chipless tag which was used to test with the reader is below 10GHz. The working frequency of the proposed reader in this dissertation is at millimeter-wave frequency range, so the reader structure would be more complicated and a better interrogation signal quality is also required. The RFID reader design is a combination of different aspects such as microwave RF design, digital signal processing and computer engineering. The objective of this dissertation is to design a reader which

is used to communicate with chipless tags. The interrogation signal is working over the millimeter-wave frequency range.

The thesis is organized in the following way:

Chapter 2 starts with the introduction of the working principle of a frequency domain based chipless MMID communication system. It carefully explains how chipless tag encodes information in the frequency domain and how reader recognizes the features of the tag. Based on the important features of a specific chipless MMID system, the detailed parameters of transmitter design would be given. A basic system knowledge including various typical system components and parameters is introduced. Some basic system concepts such as sensitivity of receiver, noise figure and 1dB compression point are also presented. In the final part of chapter 1, based on the specifications of the reader design, several different topologies of the reader structures are proposed. By comparing the advantages and disadvantages of each topology, the most suitable structure for our reader design is selected finally.

In Chapter 3, based on the selected topology of transmitter, system design consideration and simulation are applied including power budget issues, transmitted power, noise issues and loss issues. After analyzing the whole system, the design for each component is started. For the transmitted signal source design, by writing codes to control a single-chip microprocessor, both the DDS and PLL generate the desired signal. On the other hand, the active circuits in this system are all purchased commercial products. The passive circuits in this system including low pass filter, band pass filter power divider and SIW filters are presented. For the receiver of the reader, a LC bandpass filter and a VGA circuit is designed. For all the designed circuits, both simulation and test results are given. Some of the active components which are developed in the form of evaluation board from some companies are also tested to verify their performances.

In chapter 4, due to all the passive circuits in the system design are designed and tested. Two systems are fabricated and tested. The first system is a transmitter. The main reason why it need to be fabricated and tested is because the most passive circuits already designed are in the transmitter. The final transceiver system board contains both transmitter and receiver, which is also tested.

CHAPTER 2 DESIGN CONSIDERATIONS AND SYSTEM CONCEPT

2.1 Operating principle of chipless frequency domain based system

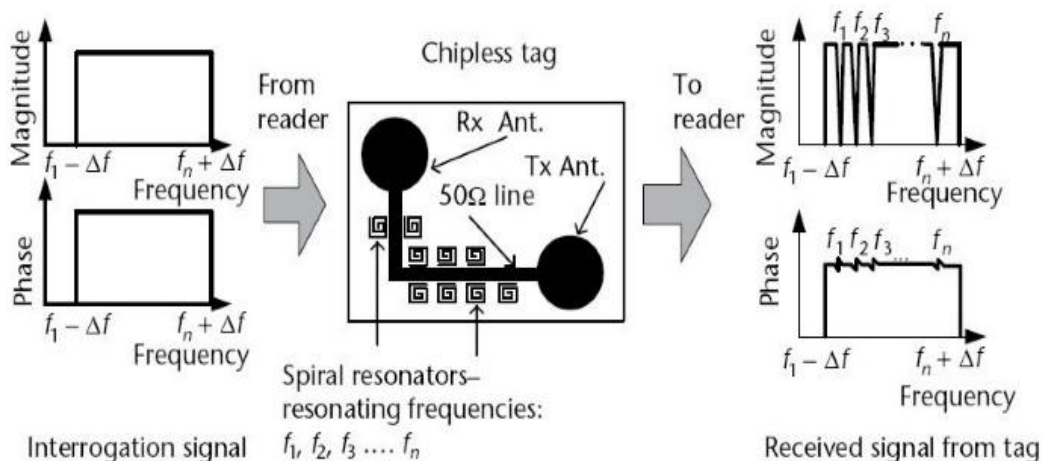


Figure 2.1. Structure and operation of a typical chipless tag encoded in the frequency domain [3].

The structure and operation of a typical chipless tag encoded in the frequency domain is shown in Figure 2.1, the tag itself is a planar microwave resonance structure with several resonators. They resonate at different frequency points or bands. Each of the resonators represents a band-stop filter [3]. When the reader sends a FMCW (Frequency-Modulated Continuous-Wave) or multi-frequency signal which could cover all the frequencies of the multi-resonating structure, the frequency signature appears. When the tag received a wideband signal, resonators start resonating at the specific frequencies and create attenuations in amplitude, it also creates phase ripples at each resonating frequency [5]. This encoded signal is then retransmitted from the tag to the reader. The frequency signature can be changed by varying the resonance frequencies. The rule to decode the information in reader is: the presence of amplitudes attenuation and phase jump is bit 0 and the absence of amplitude or phase jump at the predetermined frequency is bit 1. Figure 2.2 shows the interrogation signal of the chipless RFID system. Figure 2.3 shows the typical encoded signal of a frequency domain based chipless tag [3].

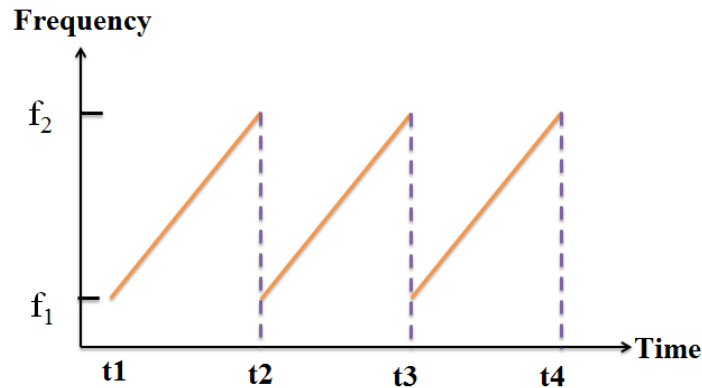


Figure 2.2. Transmitted signal in the time domain.

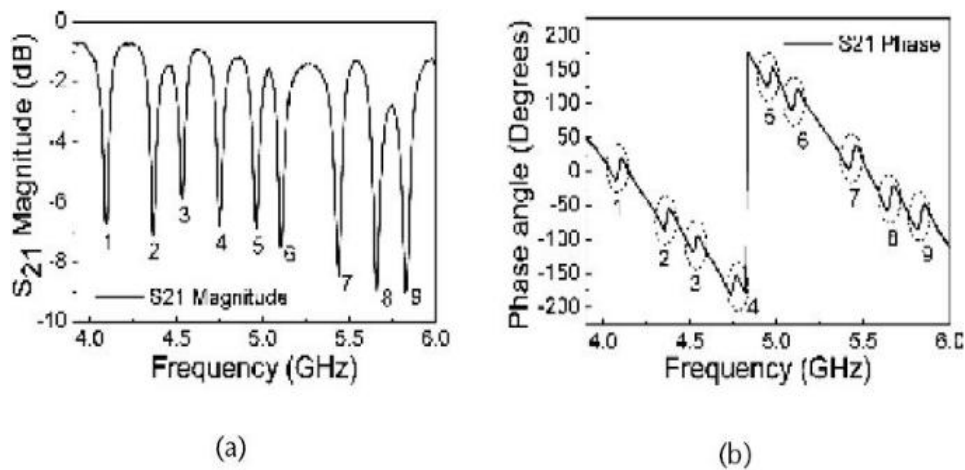


Figure 2.3. Typical encoded signal of frequency domain based chipless tag [3].

2.2 Typical circuits and system parameters in reader design

2.2.1 Antenna

Antenna is one of the essential components in a communication system [3]. Antenna is defined by Webster's Dictionary as "a usually metallic device (as a rod or wire) for radiating or receiving radio waves" [8]. The RF/microwave signal is transmitted to free space from the transmitter through the antenna. The signal propagates in free space and will be picked up by the receiving antenna. The antenna is an electrical device that converts electric power into radio waves. The antenna is widely used with transmitter or receiver. Based in different frequency ranges and on different application backgrounds, various types of antenna have been designed in recent decades. The most common types of antenna are diode antenna, horn antenna and patch antenna [9].

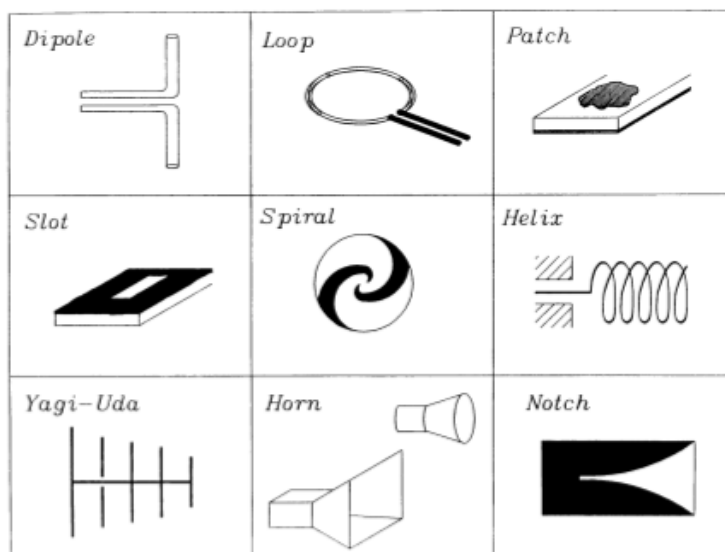


Figure 2.4. Various types of antennas in communication system [10].

2.2.2 Filters

RF/Microwave filters are used to control the frequency response at certain points in two-port networks in a RF/microwave system. Filters are two-port networks. Generally, there are four types of filters [11]: low-pass filter; high-pass filter; band-pass filter; and band-stop filter.

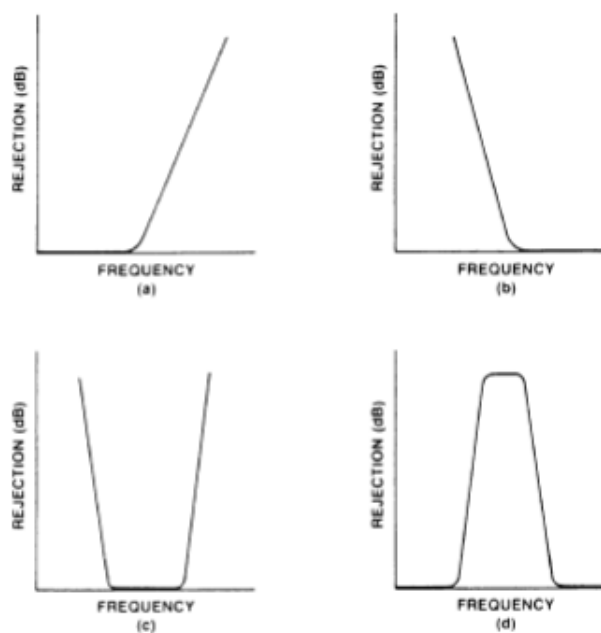


Figure 2.5. Four types of filters: (a) low-pass, (b) high-pass, (c) band-pass, (d) band-stop [10].

RF/Microwave filters are widely used in various communication systems in order to make the wanted signals go through and suppress the undesired signals. For an ideal filter, there are four features, perfect impedance matching, zero insertion loss in pass-bands, and infinite rejection in stop-bands. Maximum flat (butterworth) response and equal-ripple (Chebyshev) response are two most common designs. Planar filters such as microstrip filters or CPW filters and cavity filters, lumped-element LC filters and dielectric filters are several commonly used filters in RF or microwave frequency range[11].

2.2.3 Coupler and power divider

Power dividers and couplers are passive microwave components used for power division and combining as well as routing. Power dividers are often of the equal-division (3dB) type, but unequal power division ratios are also possible [12]. The classic types of power dividers are such as lossless T-junction power divider [13], resistive power divider and Wilkinson power divider [14].

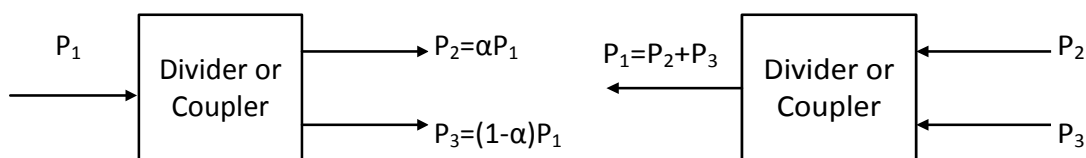


Figure 2.6. Power division and combining [12].

A coupler is a kind of passive component that is used for power division. A power divider could be a three port structure or four port structure. Both directional couplers and hybrid couplers can be made to be three or four ports based on different requirement of applications. For directional couplers, arbitrary power division can be achieved. Hybrid couplers have the same power division ratio at two output ports but phase of the two outputs differs in 90° and 180° . Circuit symbol is shown in Figure 2.7. The signal goes through to the "coupled port", the remaining signal goes to the "through port". Isolation port means that there is no power from input port to isolation in ideal situation. In practice, the isolated port has isolation of -40 dB or less. A well designed coupler should have a good VSWR, low insertion loss in each ports, good isolation and good directivity [3].

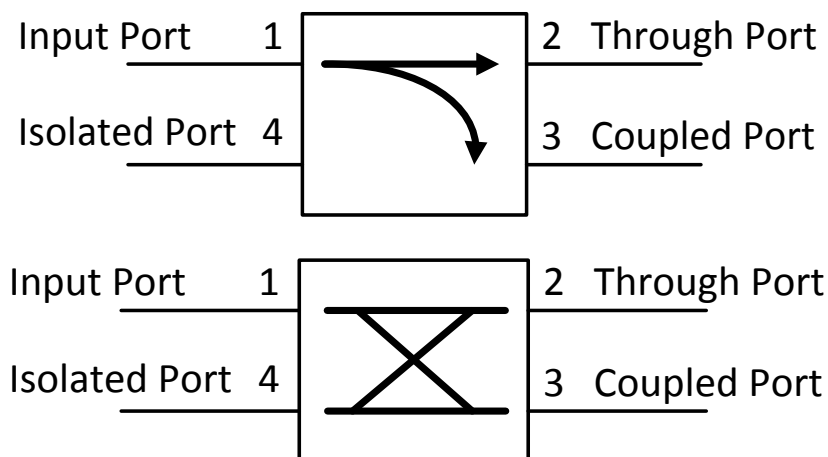


Figure 2.7. Widely used circuit symbols of coupler [3].

2.2.4 Mixer

Mixer is a three-port nonlinear device which is used to achieve frequency conversion. For an ideal mixer, the output of the mixer contains the sum and difference frequencies of its two port input signals. Diodes and transistors are typical circuits to design mixers. Because nonlinear device could generate a variety of harmonics and other products at its output, filter must be used after a mixer in microwave communication systems.

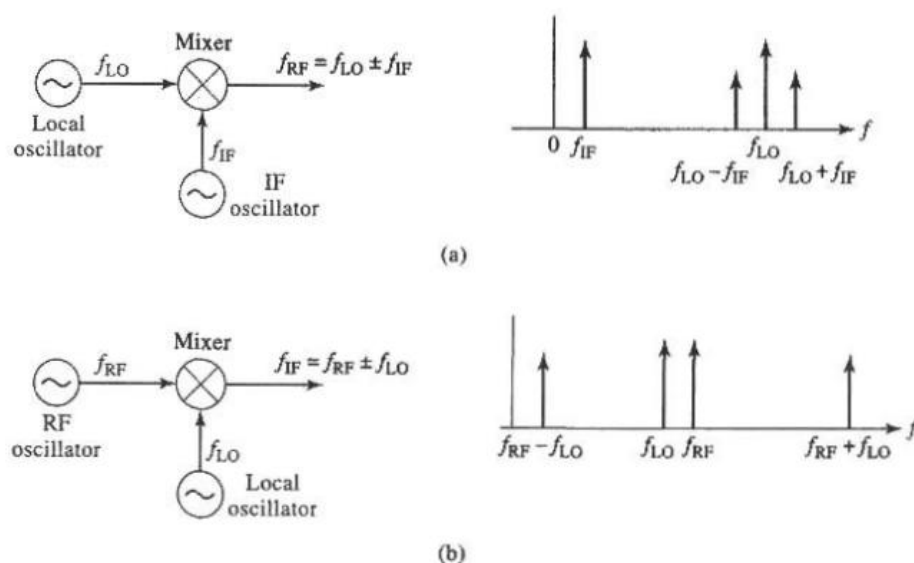


Figure 2.8. Frequency conversion with mixer. (a) Up-converter. (b) Down-converter [12].

Figure 2.8 shows a mixer used in transmitter and receiver, which act as up-converter and down-converter. The output contains the sum and difference of two input signals. There are two kinds of mixers available, active mixers and passive mixers. An external power supply is needed and they are transistor based circuits. No external power supply is needed for passive mixers and they are based on diodes [5]. A good mixer requires low conversion loss, low VSWRs for each of three ports, good isolation between any two of the RF, IF and LO ports, low noise figure, low intermodulation and high 1-dB compression point [10].

2.2.5 Amplifier

An amplifier is a kind of active component that provides power gain so it increases the power of signal. In amplifier design, the input and output matching is a key step. The important design considerations are gain, noise, and stability. The amplifier used in the last stage of a transmitter to provide high power output is called power amplifier (PA) [3]. Desired system parameters of a power amplifier are high output power, high 1-dB compression point and high third-order intercept point.

In all receivers front-end, the low noise amplifier (LNA) is the first block after the receiving antenna and microwave filter. The low noise amplifier should add noise as low as possible so that the receiver noise figure would be low. General speaking, it is not possible to achieve the best noise figure and best power gain at the same time in an amplifier design, LNA should be made with a compromise between this two targets.

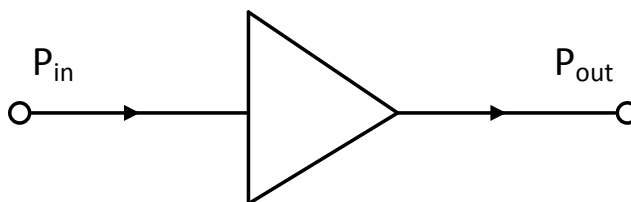


Figure 2.9. Amplifier with power gain [10].

2.2.6 VCO (Voltage controlled oscillator)

Oscillators are very important in microwave or millimeter-wave systems because they produce high-frequency signals by converting DC power into RF power. Different types of oscillators are widely used in different systems.

VCO is a kind of tunable oscillator that is widely used in different microwave and millimeter-wave systems. It changes output frequencies by a suitable control voltage. Various topologies and techniques are used to design VCOs such as piezoelectric controlled reactive elements, ferrite resonators and YIG resonator based VCOs. The most common ways to design a VCO is to use the junction capacitance of a semiconductor diode (or varactor) to realize a voltage tuning. Figure 2.11 shows a typical circuit of VCO. Low cost, less complicated implantation and wide tuning bandwidth are advantages of varactor-tuned VCOs.

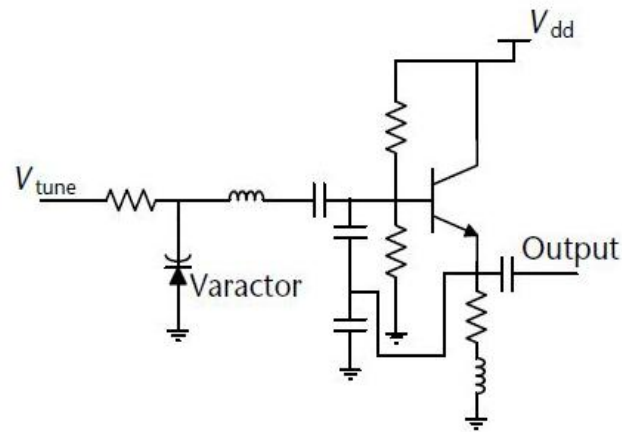


Figure 2.10. Typical schematic for a varactor based VCO [3].

There are generally two ways to generate millimeter-wave signals. One is directly using oscillators that generate signal at millimeter-wave range. The second way is to use oscillators that generate signals at low frequencies and then add frequency doubler. The final output frequency is at millimeter-wave range.

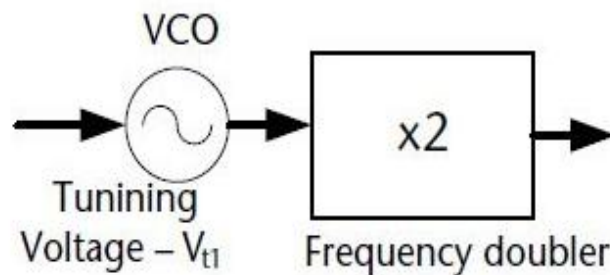


Figure 2.11. Method to generate millimeter-wave signals [3].

2.2.7 Noise figure of receiver

Noise figure is a parameter that shows how noisy a component or a system is [10]. Several aspects affect the noise figure of a component or system: losses in the circuit, bias applied and amplification. The noise factor of a two-port network is defined as

$$F = \frac{\text{SNR at input}}{\text{SNR at output}} = \frac{\frac{S_i}{N_i}}{\frac{S_o}{N_o}} \quad (2.1)$$

The noise figure is the decibel notation form of noise factor.

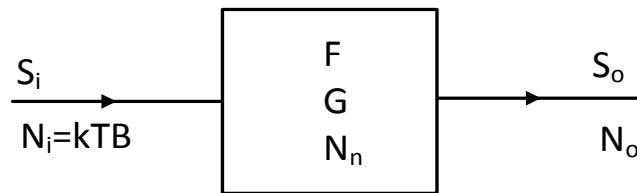


Figure 2.12. Two ports network.

Figure 2.12 shows the two-port network with gain (G). In this network and based on equation 1.1, we have

$$F = \frac{S_i/N_i}{GS_i/N_o} = \frac{N_o}{GN_i} \quad (2.2)$$

On the other hand, because

$$N_i = kT_0B \quad (\mathbf{W}) \quad (2.3)$$

where k is the Boltzmann constant, $T_0=290\text{K}$ (room temperature), and B is the bandwidth. Equation (2.2) becomes

$$F = \frac{N_o}{GkT_0B} \quad (2.4)$$

In a cascaded circuit as shown in Figure 2.9, the total noise factor affected by gain and noise factor of each circuit is

$$F = F_1 + \frac{F_2 - 1}{G_1} + \frac{F_3 - 1}{G_1 G_2} + \dots + \frac{F_n - 1}{G_1 G_2 \dots G_{n-1}} \quad (2.5)$$

According to the equation (2.5), it is obvious to see that in order to achieve a low noise factor in a system, the noise factor of the first circuit in the whole system is important. This is the main reason why in a receiver system, low noise amplifier (LNA) is at the first place [12].

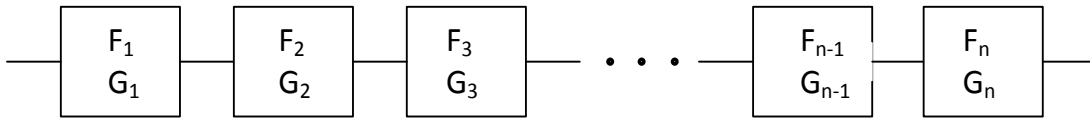


Figure 2.13. Typical cascaded circuit [12].

2.2.8 Sensitivity

The sensitivity is an important receiver parameter that shows the ability to respond to a weak signal. In other words, sensitivity is the parameter to evaluate the weakest signal that receiver could receive and process. In order to accurately describe how higher the output of the receiver compared to the output noise signal, parameter signal to noise ratio (SNR) is defined as

$$\text{SNR} = \frac{\text{wanted signal power}}{\text{unwanted noise power}} \quad (2.6)$$

Different systems have different minimum signal-to-noise ratio (SNR). For examples, 30dB for telephone lines, 40dB for TV systems and 60dB for a good music system. [10]. The sensitivity of a receiver is calculated as follow

$$S_{i,min} = KTB F \left(\frac{S_o}{N_o} \right)_{min} \quad (2.7)$$

where k is the Boltzmann factor, T is the absolute temperature, and B is the bandwidth. According to equation (2.7), we can find that in order to achieve a high sensitivity of receiver, it is necessary to lower the noise figure and narrow the bandwidth of the system.

2.2.9 1 dB compression point

In a mixer, an amplifier or a system, if one plots output power versus input power, a linear relationship will be found. The slope of the line is the gain. As the input power continues to increase, at some point the gain begins to decrease. In this situation, the response becomes non-linear and produces signal distortion, harmonics and potentially intermodulation products.

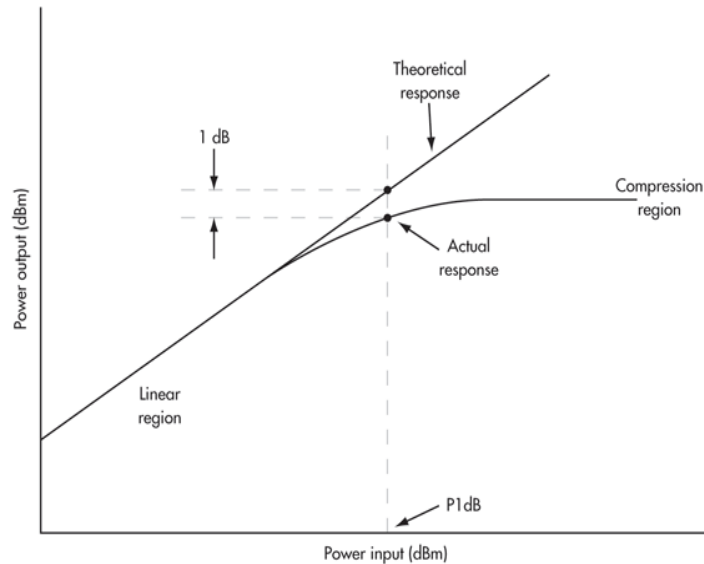


Figure 2.14. 1dB point.

The 1 dB point is the input power that causes the gain to decrease 1 dB from the normal expected linear gain plot. Operations should occur below this point in the linear region. The 1 dB compression point is important since it shows where the distortion begins in nonlinear device or system design.

2.2.10 Third-order intercept point

When two or more signals at frequency f_1 and f_2 send in a nonlinear device, IM products would be generated according to equation [10]. When m and n are in different values indicate different IM products. The third-order IM products are normally focused because in frequency domain they are very close to the desired signals.

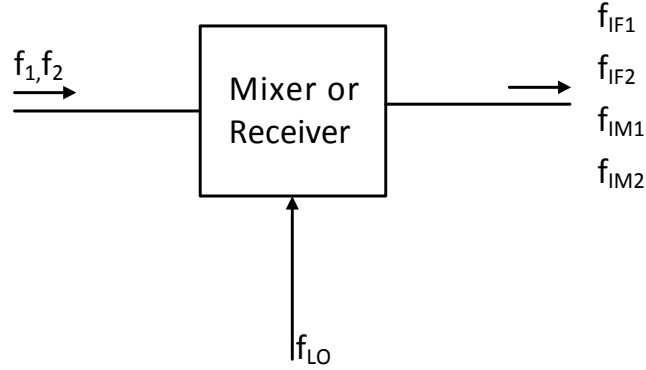


Figure 2.15. Signals generated from two RF signals [12].

In Figure 2.15, f_{IF1} and f_{IF2} are desired IF output signals in a nonlinear device. In addition, the third-order products f_{IM1} and f_{IM2} are also generated. The desired signal and nonlinear products are expressed as

$$(2f_1 - f_2) - f_{LO} = f_{IM1} \quad (2.8a)$$

$$(2f_2 - f_1) - f_{LO} = f_{IM2} \quad (2.8b)$$

$$f_1 - f_{LO} = f_{IF1} \quad (2.9a)$$

$$f_2 - f_{LO} = f_{IF2} \quad (2.9b)$$

The frequency separation is

$$\triangleq f_1 - f_2 = f_{IM1} - f_{IF1} = f_{IF1} - f_{IF2} = f_{IF2} - f_{IM2} \quad (2.10)$$

Two main reasons why these intermodulation products are usually of interest: first, they are relatively large. Second, they are difficult to suppress due to they are very close to the desired signals.

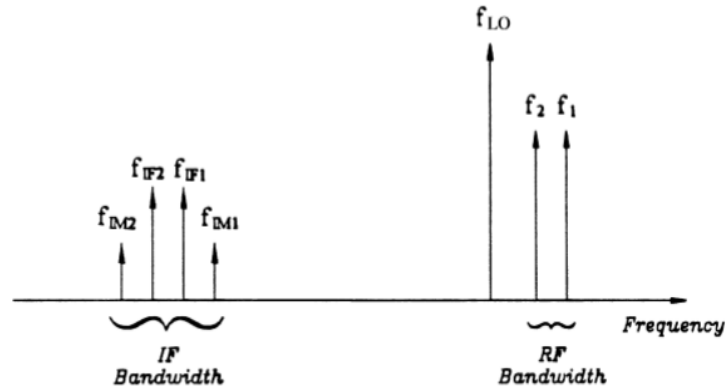


Figure 2.16. Intermodulation products [10].

Plotting the output versus input power in Figure 2.17, there are two curves in the picture, the first is the fundamental signal. 1 dB compression point occurs at one point. The other curve is the third-order product signal. These products increase at a rate three times of the fundamental signal curve.

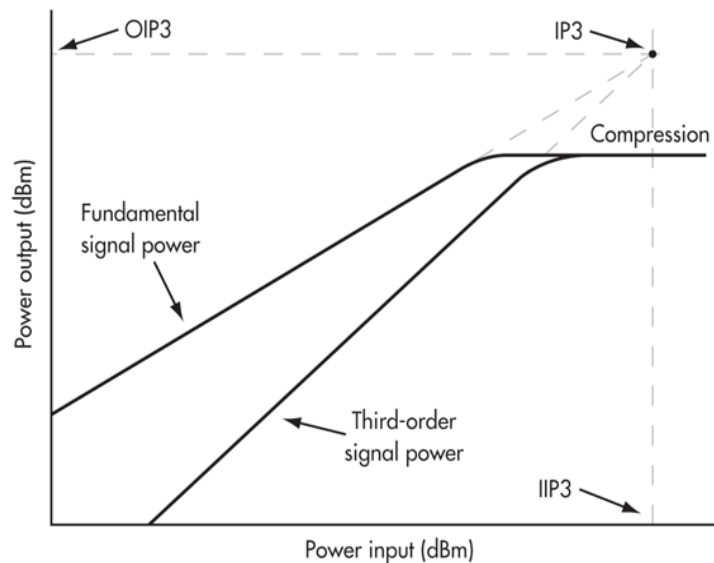


Figure 2.17. Relation between 1 dB compression point and IP3 point.

If extending two curves, they will finally meet at a point where the third-order signal power is equal to the fundamental signal power. This theoretical point is called third-order intercept point (IP3). The IP3 value essentially indicates how large a signal the amplifier can process before intermodulation distortion (IMD) occurs.

2.3 Three methods to generate FMCW signal

Direct digital synthesis (DDS) is a type of frequency synthesizers used to produce arbitrary analog waveform by generating a time-varying signal in digital form and then making a digital-to-analog conversion. DDS has the advantages of fast frequency switching speed and fine frequency resolution.

Phase-locked loop (PLL) is another type of frequency synthesizer that could achieve good frequency stability and low phase noise. A typical PLL consists of a stable frequency oscillator which acts as the reference source, a phase detector, a low-pass filter, a VCO and a frequency divider.

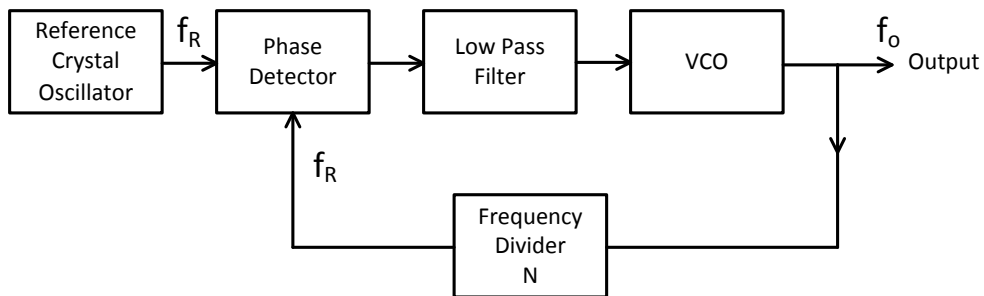


Figure 2.18. A typical PLL.

To start with the reader design, the first thing is determining how to generate the wideband signal. Generally, there are three methods to generate a wideband signal.

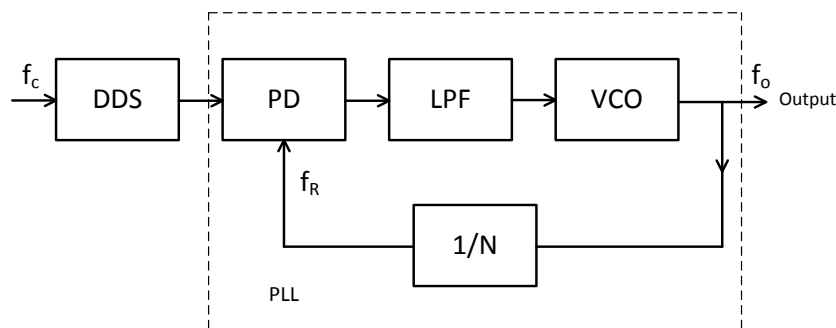


Figure 2.19. First method to generate wideband signal with DDS and PLL.

In the first method, the reference signal of PLL is the output signal of DDS. DDS generates a wideband signal to the input of PLL. As a result, the PLL will also output a wideband signal. The disadvantage of this method is that for PLL module, frequency lock-in time is at ms (millisecond) level. For a fast sweep of DDS, time step could be at 10-100 ns (nanosecond) level, so a lost frequency

locking could cause the serious phase noise deterioration of final output signal from PLL. Figure 2.19 shows the schematic diagram of the first method.

In Figure 2.20, PLL works as a high quality local oscillator signal. Wideband signal is also generated by DDS. The frequency resolution and frequency switching time of the wideband signal are controlled by DDS itself. Compared to the first method, this case could achieve a better output frequency quality due to the fact that the output of DDS does not go through the PLL so the spurious and phase noise are not worse.

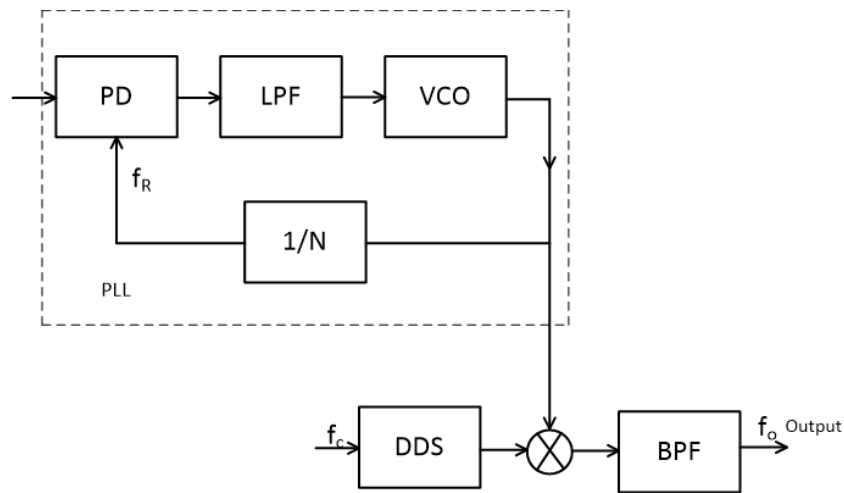


Figure 2.20. PLL and DDS mix up to generate wideband signal.

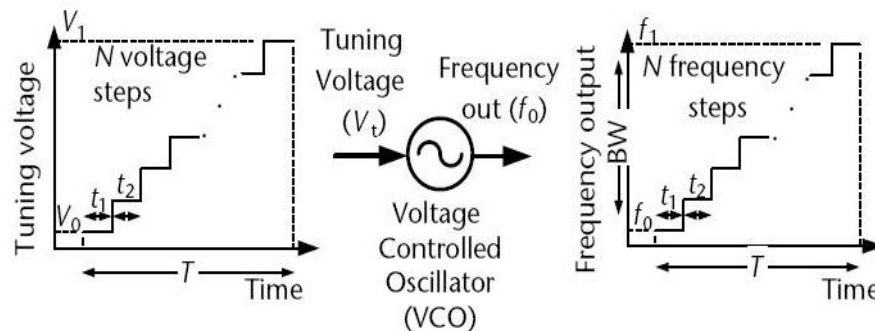


Figure 2.21. Generation of a wideband frequency signal using a VCO [3].

The third method is also adopted in [15], such a wideband signal can be generated using a VCO as shown in Figure 2.21. The frequency output of the VCO varies from f_1 to f_2 , generating a frequency sweep with a constant amplitude of wideband microwave power when DAC generates discrete voltage steps with very small voltage steps at the input of VCO. The advantage of this method is the simple structure. But the disadvantage of this structure is that compare to the output signal of

DDS, the quality of a wideband signal generated by VCO is worse than DDS such as strong spurious signals and high phase noise.

After comparing the three methods, considering achieving a high quality interrogation signal and having a structure as simple as possible, the second method is selected.

In this reader design, a 35-36GHz wideband transmitted signal should be generated for a chipless MMID tag.

2.4 Different reader topologies comparison

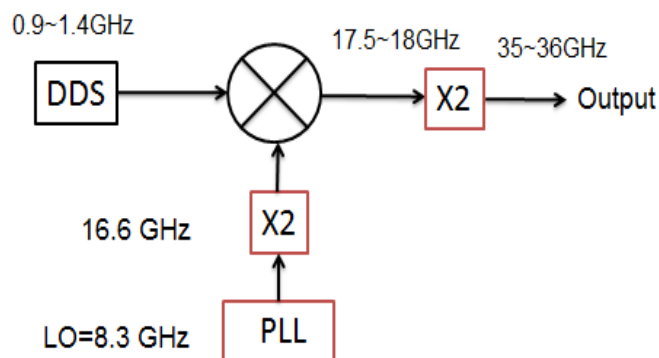


Figure 2.22. First topology of the transmitter.

Based on the fact that in all the following four topologies, the output signal qualities of PLL and DDS are the same. Figure 2.22 shows the first topology of transmitter design. The first topology is the same as that in [16]. There are two multipliers in this topology. The output of mixer will be doubled one time so that the output frequency will be at 35-36 GHz.

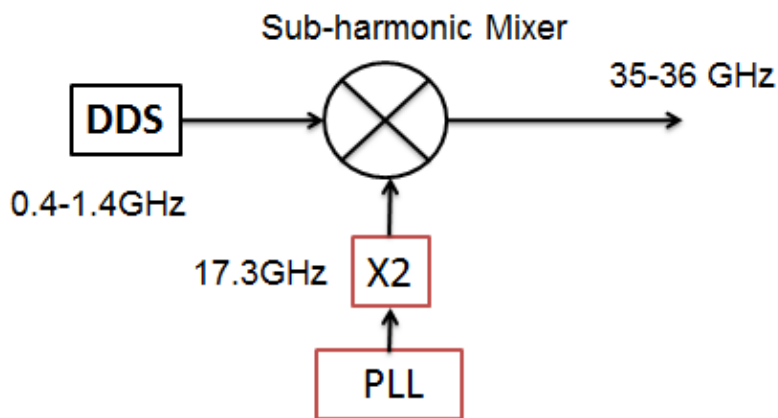


Figure 2.23. Second topology of the transmitter.

Figure 2.23 shows the second topology of transmitter, the advantage of the second topology is the simple structure, a frequency multiplier (double) of the PLL output signal, the sub-harmonic mixer could directly generate a 35-36 GHz wideband signal.

Because of the maximum output frequency of DDS 9914 is 1.4 GHz, the disadvantage is that it is hard to design such a band-pass filter that is able to suppress undesired signal generated by sub-harmonic mixer. Figure 2.24 shows the output signal in frequency domain, we can see that around 35 GHz, the frequency range between desired wideband signal and 2LO signal is only 400 MHz, the frequency range between the desired signal and undesired signal is only 800 MHz. It is too difficult to design a filter that could effectively suppress 2LO and other signals in such short frequency distance.

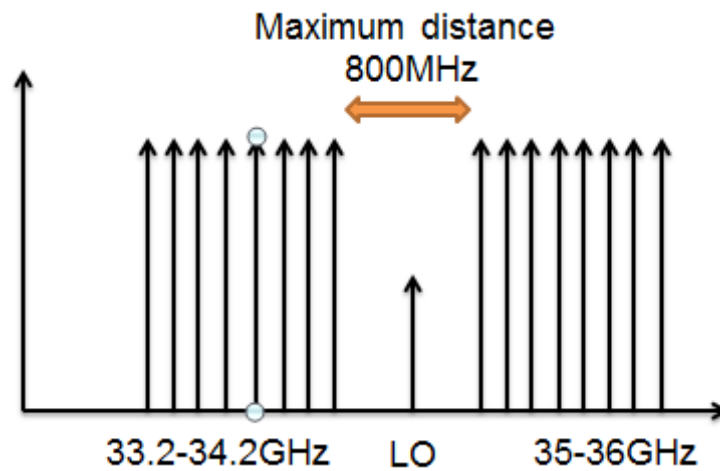


Figure 2.24. Output signal of sub-harmonic mixer in second topology.

The third topology is shown in Figure 2.25. Two mixers and two PLL are applied in this topology. With a comparison of topology 1 and 2, the first topology is easier to design. When comparing topology 1 and 3, the structure of first topology is more compact. So the first topology is selected due to its compact structure, good stability and signal quality.

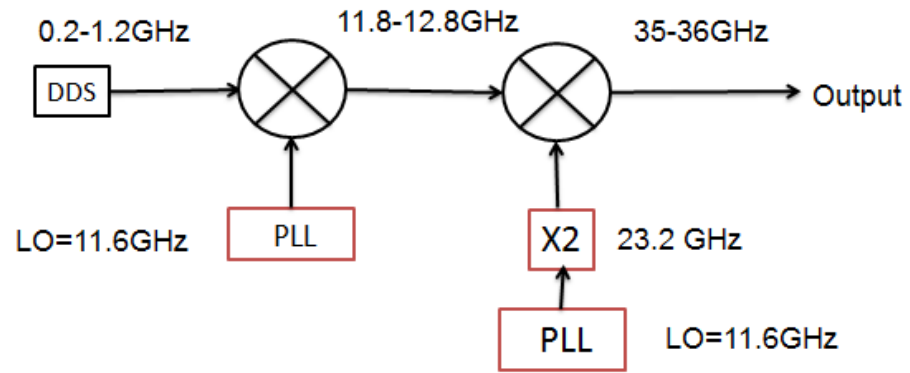


Figure 2.25. The third topology of transmitter.

CHAPTER 3 SYSTEM SIMULATION AND CIRCUITS DESIGN

3.1 System simulation

Based on the system topology analysis in the first chapter, the specifications of system and the reader structure could be determined in Table 3.1 and Figure 3.1, respectively.

Table 3.1. Specifications of our proposed reader design.

Specifications	Values
Frequency range	35-36GHz
Maximum channel bandwidth	1 GHz
Maximum output power	1 W (30dBm)
Output signal	FMCW signal
Working Distance	3-10 m

Based on the basic system knowledge introduced in the first chapter, assuming that the noise figure of the receiver is 5 dB and the minimum output SNR is 15 dB, and the bandwidth $B = 2\text{MHz}$, according to equation (2.7), the sensitivity of the receiver is -91 dBm.

On the other hand, a chipless MMID tag in [17], coded in frequency domain is designed and measured. The measurement method is shown in Figure 3.2. The measured result is shown in Figure 3.3.

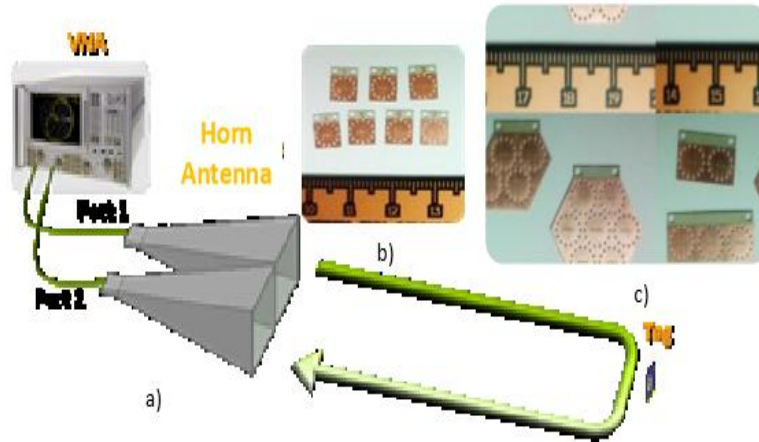


Figure 3.1. Measurement set up for chipless MMID tag [17].

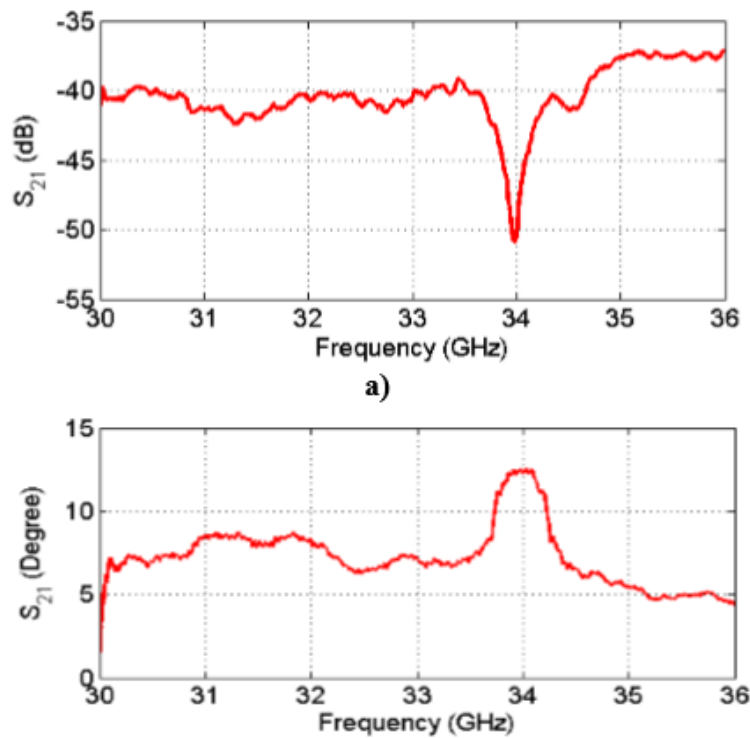


Figure 3.2. Measured results of chipless MMID tag [17].

In [6], the distance between VNA antenna and chipless MMID tag is 30 cm, the two antenna gains are both 20 dBi. So for the total 60 cm distance transmission distance, the whole loss is -40 dB. This loss includes the loss on the tag and loss in free space.

On the other hand, according to Friss equation (3.1), the loss of 35 GHz signal over the 60 cm distance is -19 dB. So the loss on the tag is approximately -20 dB. Finally, using the radar equation

(3.2), the maximum working distance between the reader and the tag is 30 m. It proves that the 3 m working distance is realizable.

$$P_r = \frac{G_t G_r \lambda_0^2}{(4\pi R)^2} \quad (3.1)$$

$$R_{max} = \left[\frac{P_t G^2 \sigma \lambda_0^2}{(4\pi)^3 K T B F \left(\frac{S_o}{N_o} \right)_{min}} \right]^{\frac{1}{4}} \quad (3.2)$$

According to the system comparison in Chapter 1 and the specifications of the reader in Chapter 2, the final architecture of our reader design is shown in Figure 3.3. Table 3.2 shows the determined circuits in the proposed system.

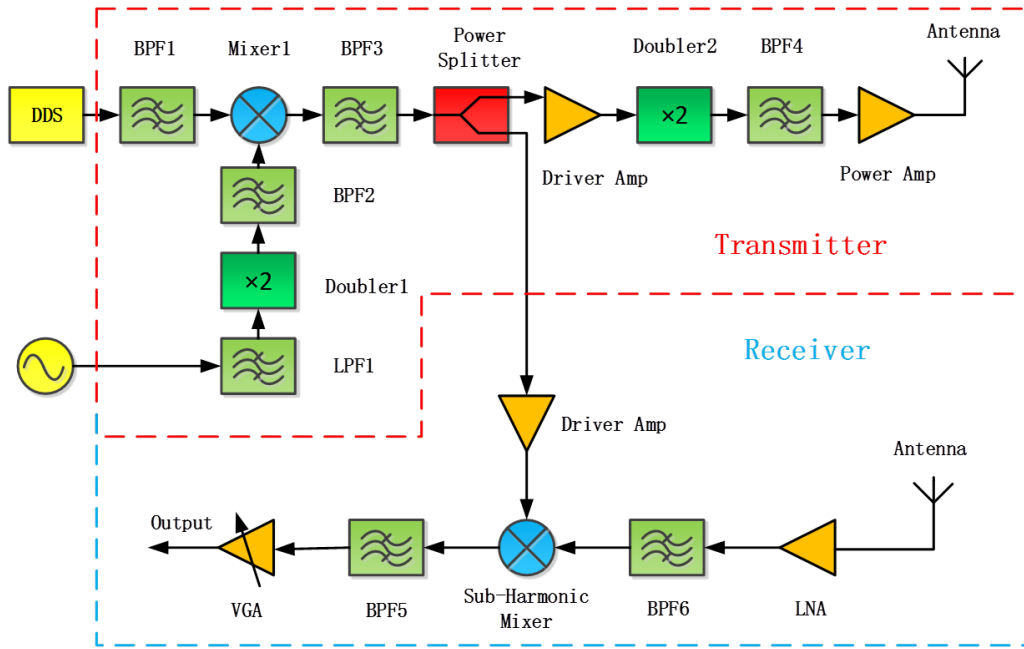


Figure 3.3. Proposed reader structures for chipless MMID tag.

Firstly, the wideband signal is generated by both DDS and PLL, the frequency range of output DDS is 0.9-1.4GHz. The output frequency of PLL is 8.3 GHz. The output of PLL will first be doubled in frequency domain so a 16.6 GHz LO signal will be sent to the mixer. After mixing, a 17.5-18 GHz wideband signal is generated. A power divider is applied after the mixer to separate the signal so that one way is used as the transmitted signal and the other is used as the LO signal

of the down converter in the receiver. The transmitted signal will be doubled again so that the 35-36 GHz wideband signal would finally be generated.

In the receiver side, after filtering and amplifying, a small signal would be processed by a sub-harmonic mixer. The signal will finally be processed in VGA.

Table 3.2 Components and their realizations of transmitter

Component	Realization	Component	Realization
DDS	AD 9914	Power Amplifier	HMC 635
PLL	HMC 765	Gain Block	HMC 451
Lowpass filter1	Step-impedance filter	Mixer	HMC773
Lowpass filter2	XLF-192+ (mini circuits)	Power Divider	Wilkinson PD
Bandpass filter1	Wideband Filter	Multiplier 1	HMC 573
Bandpass filter2	SIW filter	Multiplier 2	HMC 579
Bandpass filter3	SIW filter		

Table 3.3 Components and their realizations of receiver

Component	Realization	Component	Realization
LNA	HMC 1040	Bandpass Filter	LC Lumped Filter
Gain Block	HMC 451	VGA	AD8338A
Sub-harmonic Mixer	HMC 339		

Table 3.2 and Table 3.3 summarize various circuits of the whole transceiver system. All the passive circuits are free samples donated by Hittite. All the passive circuits except low-pass filter 2 are designed by us.

Finally, the system simulation is executed and completed in ADS (Advanced Design System) in system budget simulation mode. ADS is the world’s leading electronic design automation software for RF, microwave applications. The Budget controller enables to perform an RF system budget analysis to determine the linear and nonlinear characteristics of an RF system. The results are shown in Table 3.4 and Table 3.5.

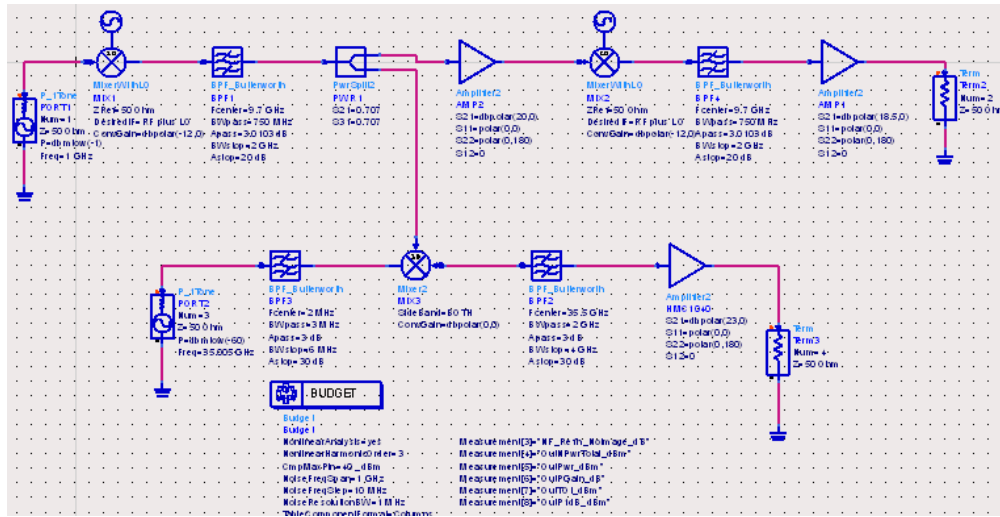


Figure 3.4. System simulation in ADS.

Table 3.4. System simulation results of transmitter.

	HMC773	BP filter	Power divider	HMC451	HMC579	BP filter	HMC635
Component Gain	-12 dB	-3 dB	-3dB	19 dB	8 dB	-4 dB	18.5dB
System Gain	-12 dB	-15 dB	-18 dB	1 dB	9 dB	5dB	23.5 dB
Output Power	-13 dBm	-16dBm	-19dBm	0dBm	8dBm	4dBm	22.5dBm
P1dB	-2 dBm			30dBm			22dB

Table 3.5. System simulation results of receiver.

	HMC1040	SIW Filter	HMC 339	LC Filter	VGA
Component Gain	23 dB	-4 dB	-12 dB	-0.5 dB	50 dB
System Gain	23 dB	20 dB	8 dB	7.5 dB	57.5 dB
Component NF	2.2 dB	4 dB	-10 dB	0.5 dB	5 dB
System NF	2.2 dB	2.22 dB	2.5 dB	2.56 dB	
Output Power	-37.013 dBm	-41.013dBm	-53.015dBm	-53.515dBm	-3.54dBm

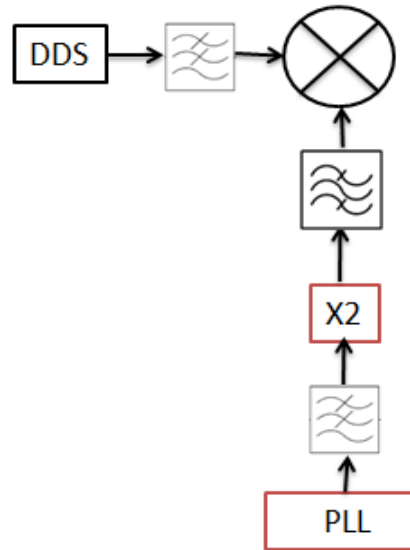


Figure 3.5. Signal source of transmitter.

3.2 Circuits design of reader system

The first part of the system design is the signal source of the transmitter. AD9914 generates a wideband signal from 0.9-1.4 GHz. After the output of AD9914, a LC low-pass filter is used to suppress the spurious signal of the output of AD9914. At the input of the LO of the mixer, PLL generates a single tone signal which output frequency is 8.3 GHz. The stepped-impedance filter is used to suppress harmonic signals of the output of HMC765, then multiplier HMC 573 is used to double the frequency of 8.3 GHz. A wideband band-pass filter after HMC 573 is used to suppress the harmonic frequencies of HMC573.

3.2.1 AD 9914 (DDS)

D9914 is a direct digital synthesizer (DDS) featuring a 12-bit DAC. AD9914 also supports a user defined linear sweep mode of operation for generating linear swept waveforms of frequency, phase, or amplitude. A high speed 32-bit parallel data input port is included, enabling high data rates for polar modulation schemes and fast reprogramming of the phase, frequency, and amplitude tuning words.

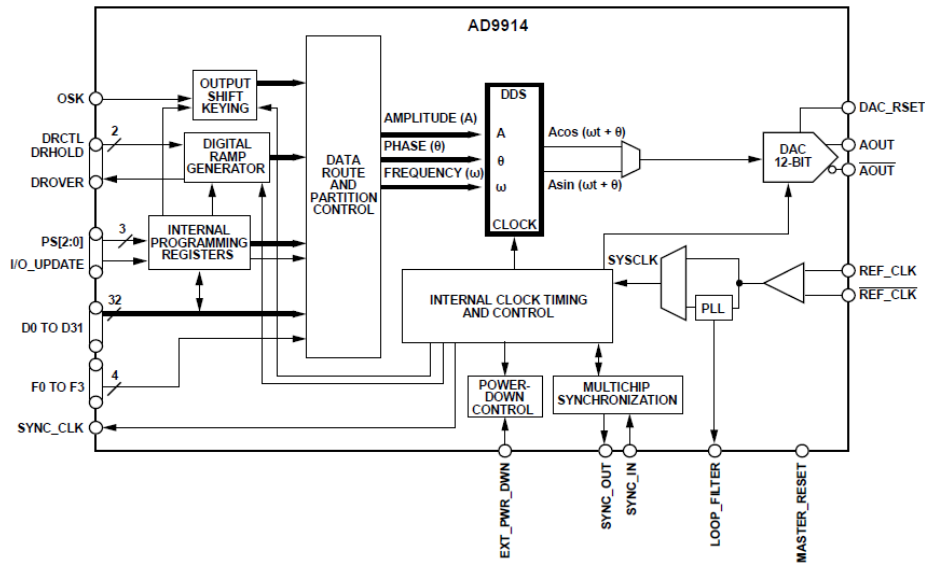


Figure 3.6. Internal structure of AD9914.

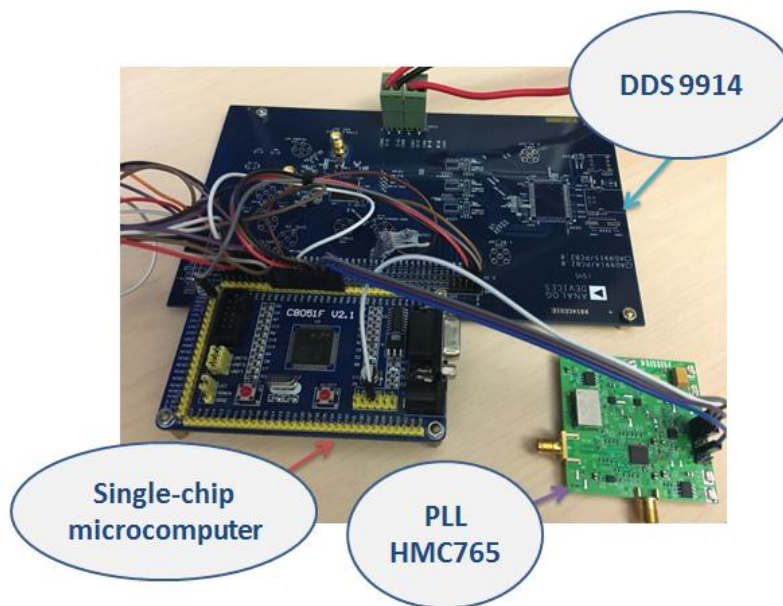


Figure 3.7. Evaluation boards of HMC765 and DDS9914.

3.2.2 HMC765 (PLL)

HMC765 is a fully featured Fractional-N Phase-Locked-Loop (PLL) with an Integrated Voltage Controlled Oscillator (VCO). The input reference frequency range is from 100 kHz to 220 MHz while the advanced modulator design in the fractional PLL allows both ultra-fine step sizes and very low spurious products. The output frequency range is from 7.8 to 8.8 GHz,

In this system, it is necessary to write codes with single-chip microcomputer so to control the evaluation board of HMC765 and AD9914 simultaneously. Test result of HMC765 is shown in Figure 3.8.

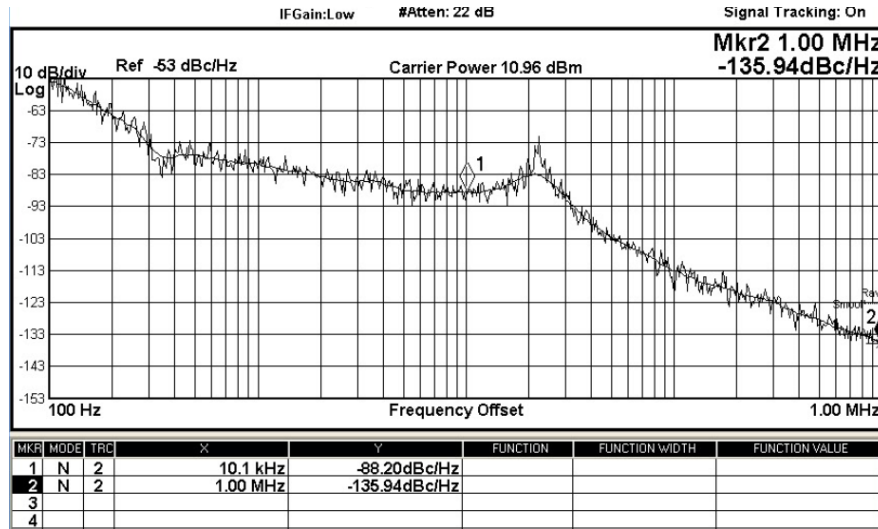


Figure 3.8. Phase noise of output signal generated by HMC765.

3.2.3 Microstrip line and ground coplanar waveguide (GCPW)

Before starting with each circuit design, it is necessary to determine the type of transmission line used in this reader system.

Microstrip line is the most common and popular transmission line in microwave circuits and system design due to its simple structure, easy fabrication and easy integration.

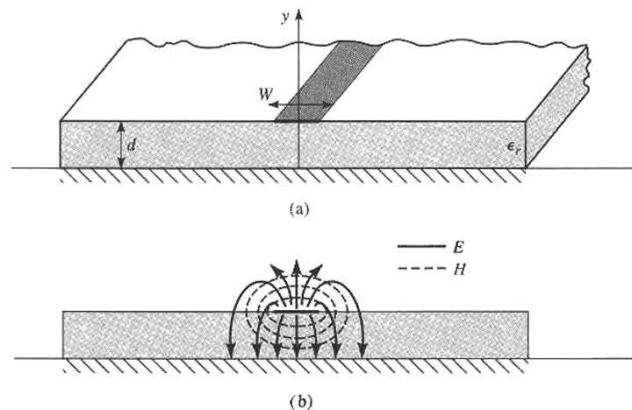


Figure 3.9. Microstrip line [12].

Grounded coplanar waveguide (GCPW) is another strip transmission line. The geometry of GCPW is shown in Figure 3.10. The signal conductor is designed between two ground conductors all on the top of the dielectric layer. An additional ground plane is on the bottom of the dielectric layer. In order to achieve a consistent ground performance, conductive-metal-filled via-holes or slots connect to the top-layer and bottom-layer of the ground plane.

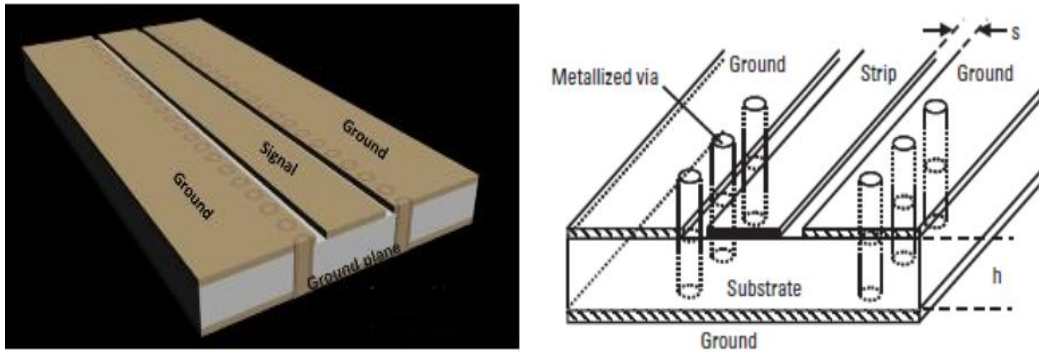


Figure 3.10. GCPW transmission line.

When frequency increases to millimeter wave frequency band, the grounded coplanar waveguide (GCPW) is capable of lower loss than microstrip line due to its special ground structure. Microstrip structure suffers from increased circuit losses over the millimeter-wave frequency range, making the circuit technology less efficient for use at frequencies of 30 GHz or higher. GCPW structure is adopted as the transmission line in this reader design. The structure of the GCPW is shown in Figure 3.10. In this system design, RT/Duroid 6002 from Rogers Corporation is selected as the system PCB board due to its good characteristics in the high-frequency range. The thickness of the PCB board is 0.254 mm (10mil).

3.2.4 Stepped-impedance low-pass filter

Since the output signal of PLL is the desired frequency signal as well as its harmonic frequencies, a low pass filter is needed to suppress the undesired output signals of the PLL. Stepped-Impedance low pass filter is a good choice because this filter is easier to design and takes up less space than other low pass filters with stubs.

Based on the design rule in [12], a six-order stepped-impedance low pass filter is designed and tested. The specifications of this filter are: cutoff frequency of 9 GHz, impedance of 50 ohms, the highest practical line impedance is 120 ohms, the lowest is 20 ohms. Both simulation and test

results show that this filter suppresses the undesired frequency signal well. The size of the filter is shown in Table 3.6. “W” means the width of the steps and “L” means the length of the steps.

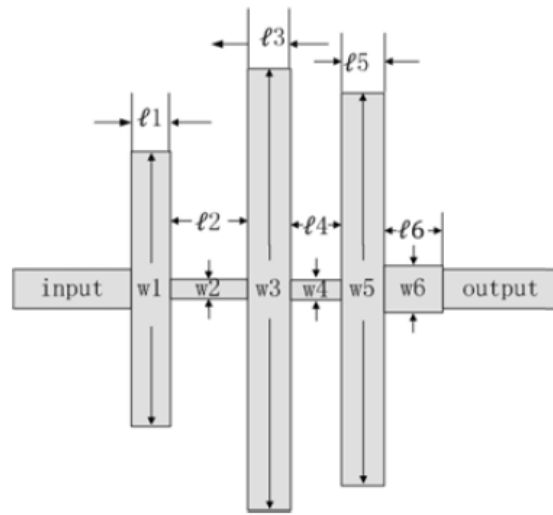


Figure 3.11. Geometry of the six-order stepped-impedance low-pass filter.

Table 3.5 Dimensions of the six-order stepped-impedance low-pass filter

Width	Value (mil)	Length	Value (mil)
W1	184.5	L1	10.8
W2	20	L2	114.8
W3	300	L3	10
W4	6	L4	53.6
W5	250	L5	10
W6	6	L6	16.5

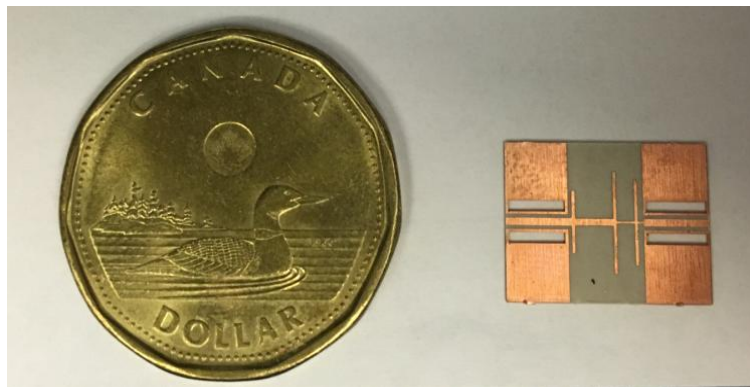


Figure 3.12. Fabricated stepped impedance low pass filter.

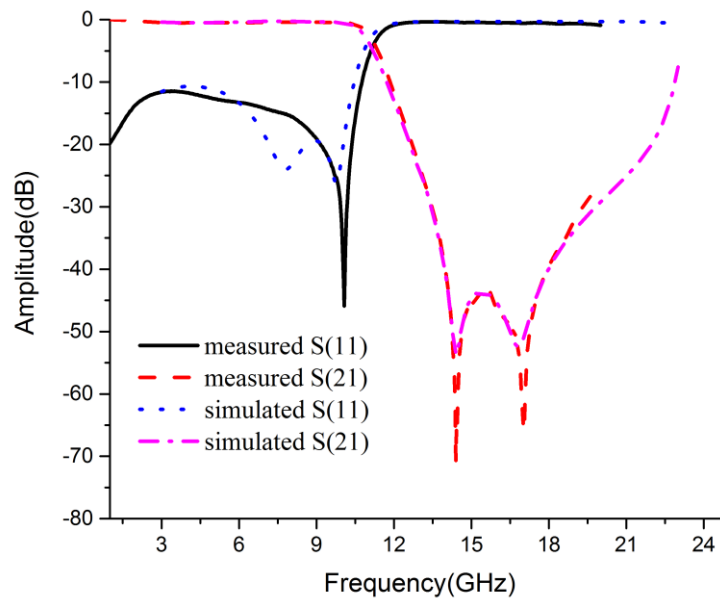


Figure 3.13. simulation and test results of the stepped-impedance low-pass filter.

Both simulation and test results are shown in Figure 3.13. In the simulation results, the insertion loss at 8.3GHz is -0.3dB, the insertion loss at 16.6GHz is -47 dB. The return loss at 8.3GHz is -21.5 dB. In the test results, the return loss at 8.3 GHz is -17.7 dB and insertion loss at 8.3 GHz and 16.6 GHz are -0.4 dB and -46 dB respectively. So this stepped impedance filter effectively suppresses the second harmonic signal of the output of PLL.

3.2.5 HMC573 (Multiplier)

HMC573 is a x2 active broadband frequency multiplier. The output frequency range is from 8GHz-22GHz. The low additive SSB phase noise of -134 dBc/Hz at 100 kHz offset helps maintain a good system noise performance.

The test result of the evaluation board of HMC573 is shown in Figure 3.14. It shows that not only $2f_0$, but f_0 , $3f_0$ and $4f_0$ are also generated at the output of HMC573. So a band-pass filter is needed here to suppress the undesired frequency signals which are f_0 , $3f_0$ and $4f_0$ in this case.

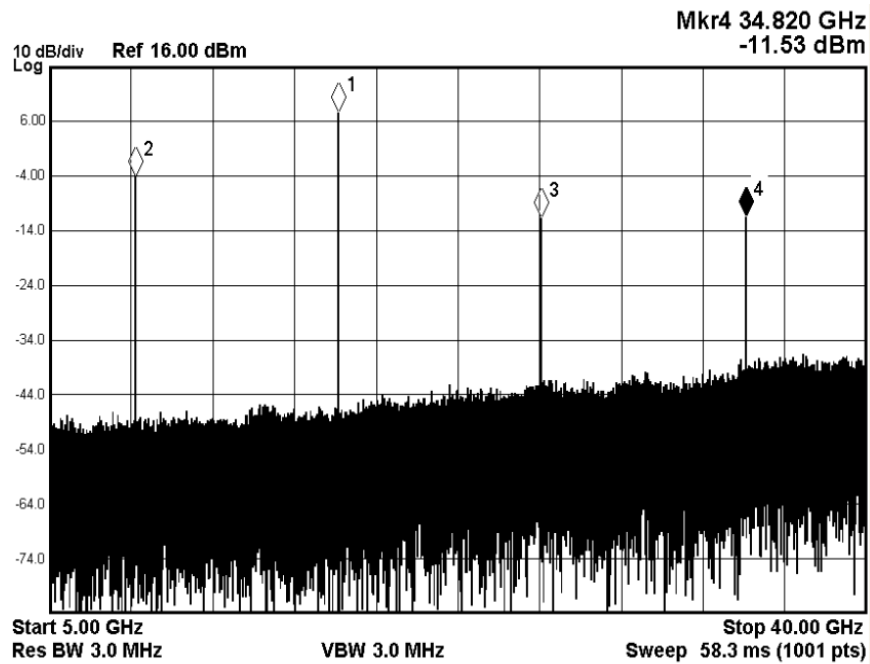


Figure 3.14. Test result of HMC573.

3.2.6 Band-pass filter design

The test result of frequency multiplier HMC573 shows that many harmonic frequencies are also generated by the frequency multiplier. So a band-pass filter is needed to effectively suppress the harmonic frequencies of the output of HMC573. In [18], a wideband band-pass filter is designed. Since an SIW transmission line can be treated as a high-pass filter, an SIW transmission line combining with a stepped-impedance low pass filter would make up a band-pass filter. The six-order stepped impedance low pass filter and an SIW transmission line are designed and simulated in HFSS, respectively. A final combined band-pass filter is then fabricated.

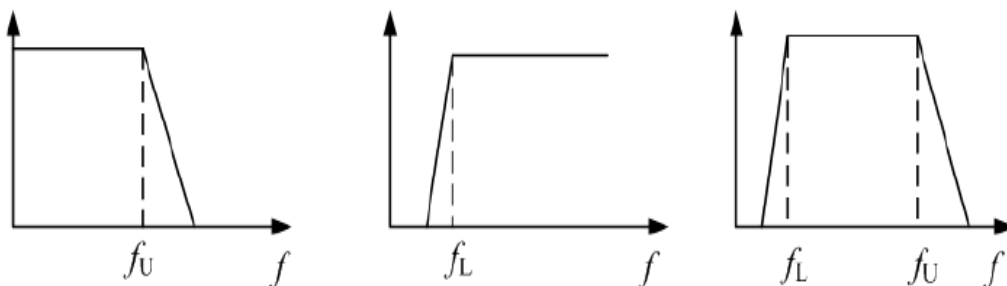


Figure 3.15. The schematics of the forming process of a wide-band band-pass filter[18].

Table 3.7 shows the dimensions of the six-order stepped impedance low pass filter, and Figure 3.17 shows the simulated results of the designed six-order impedance low-pass filter.

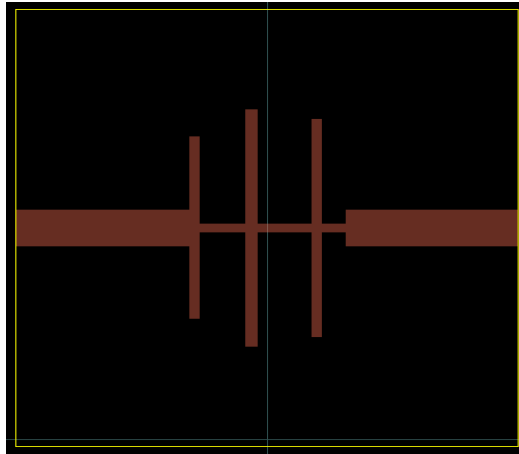


Figure 3.16. Designed six-order stepped impedance low pass filter.

Table 3.6 Dimensions of the six-order stepped-impedance low-pass filter

Width	Value (mil)	Length	Value (mil)
W1	127.2	L1	6
W2	6	L2	24.6
W3	180	L3	6
W4	6	L4	28.8
W5	156	L5	6
W6	6	L6	14.3

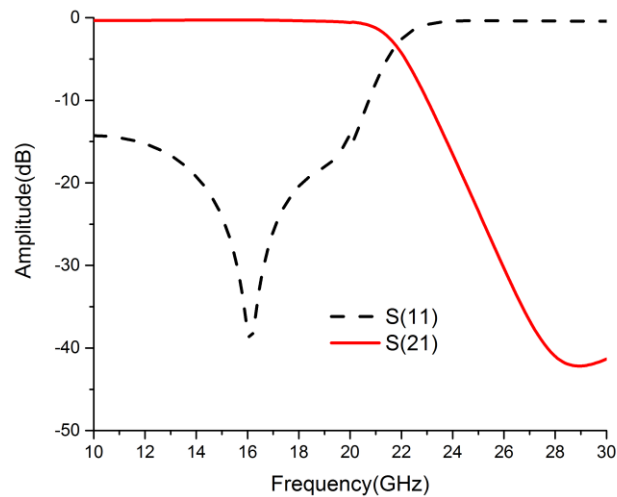


Figure 3.17. Simulation results of the stepped impedance low pass filter.

It has been well known that substrate integrated waveguides (SIWs) are integrated waveguide-like structures fabricated by using two rows of conducting cylinders or slots embedded in a dielectric substrate that electrically connect two parallel metal plates [19]. In this way, a non-planar rectangular waveguide can be made in planar form. The propagation characteristics of SIW structures are similar to the classical rectangular waveguides.

There are many advantages when using this technique such as the reduction of system size, lower cost and easy to fabricate. The most advantage of using such a method is that enables all the components on the same substrate. Various passive and active SIW circuits have been developed such as filters [20], directional couplers [21], oscillators [22], power amplifiers [23] and antennas [24]. Figure 3.18 shows the geometry of an SIW structure.

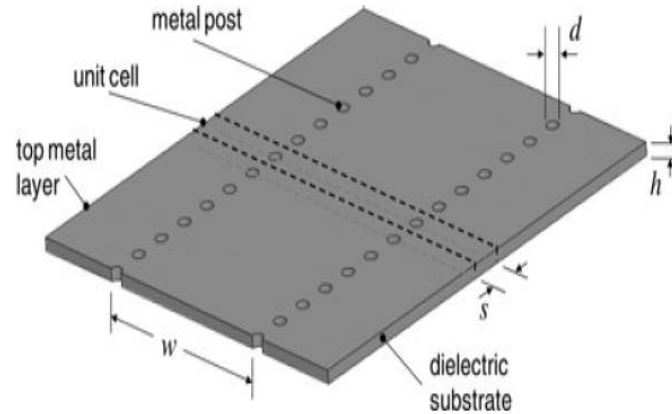


Figure 3.18. Geometry of an SIW [19].

In order to integrate SIWs and other planar circuits, different SIW-planar structure transitions are developed such as SIW-microstrip line connection and SIW-CPW connection. The design of the SIW-microstrip transition is straightforward. A taper is used to excite the waveguide mode. The performance is excellent to cover entire SIW bandwidth. On the other hand, CPW or GCPW is a preferred transmission line in the millimeter-wave range. In this system design, the SIW-GCPW transitions are used for two SIW filters design [25].

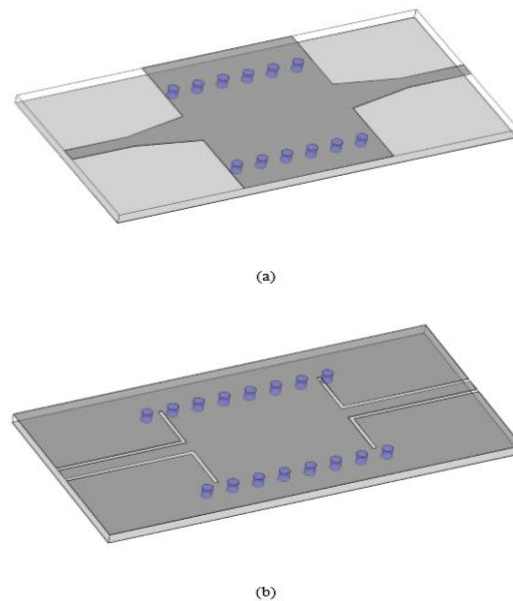


Figure 3.19. Two transitions from planar circuits to SIW (a) microstrip line, (b) conductor backed CPW line [25].

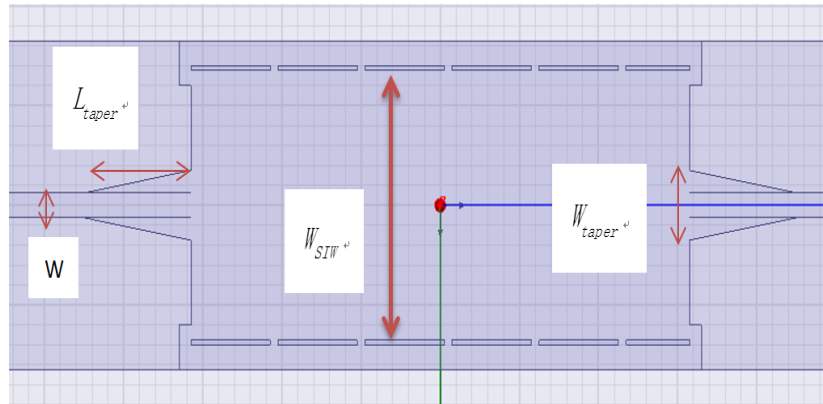


Figure 3.20. Structure of SIW transmission line.

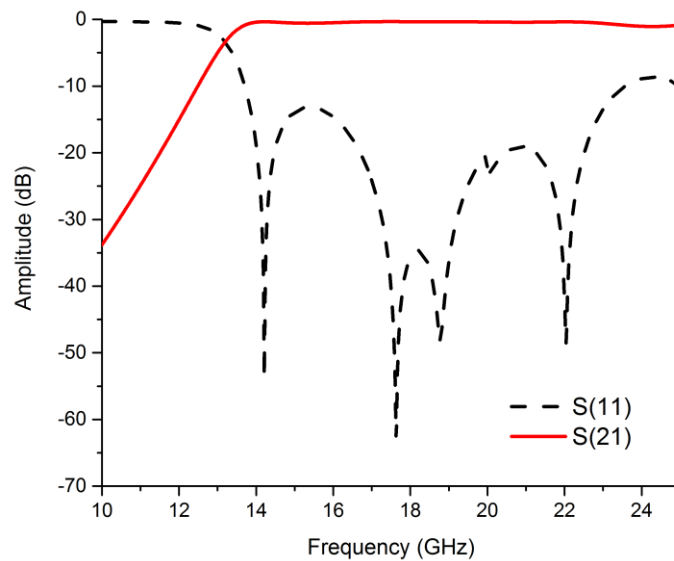


Figure 3.21. Simulated results of an SIW transmission line.

In Figure 3.20, the structure of the designed SIW transmission used as the high-pass filter is presented. In Figure 3.20, W_{SIW} is the width of the SIW transmission line, W_{taper} and L_{taper} are the width and length of the taper, respectively. W is the width of the 50 Ohms transmission line. In this design, $W_{SIW}=270\text{mil}$, $W_{taper}=22.6\text{mil}$, $L_{taper}=135\text{mil}$ and $W=24.8\text{mil}$. The distance between two ground slots are 10mil. Simulated results of the high-pass filter are shown in Figure 3.21.

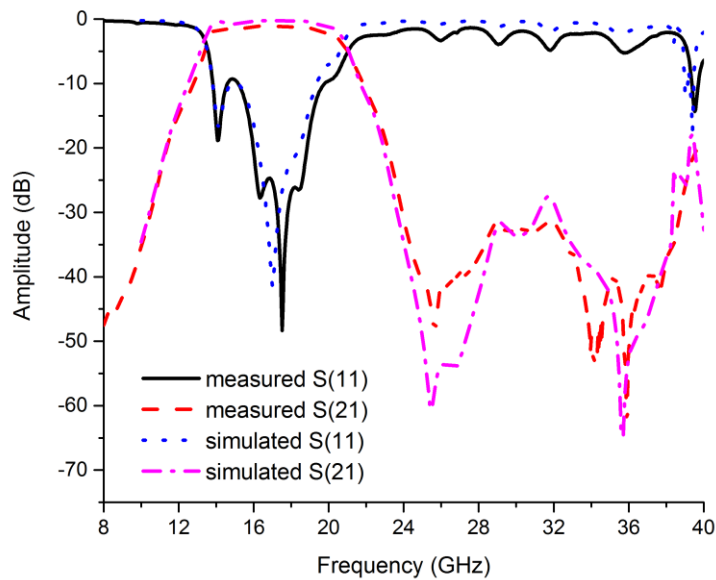


Figure 3.22. Simulated and measured results of the wideband band-pass filter.

Measured and simulation results of the wideband band-pass filter are shown in Figure 2.22. In the test result, the insertion loss at 16.6 GHz is -1.1 dB whereas the insertion loss at 8.3 GHz, 24.9 GHz and 33.2 GHz are all under -40 dB. The return loss at 16.6 GHz is under -20 dB. The measured results are well matched with the simulated results.

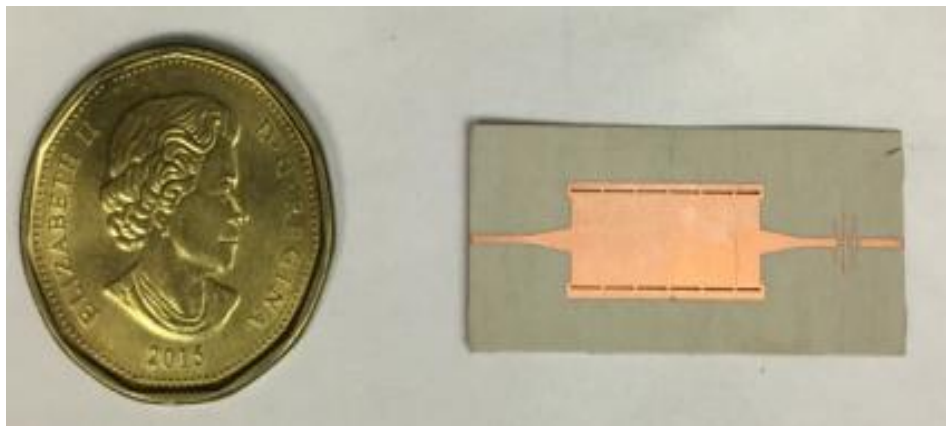


Figure 3.23. Fabricated wideband band-pass filter.

3.2.7 Low-pass filter after AD9914

In order to suppress spurious of AD 9914, a low-pass filter sample named XLF-192+ is obtained from Mini-circuits. The pass band is from DC-1.9GHz. Measured result is shown in Figure 3.24.

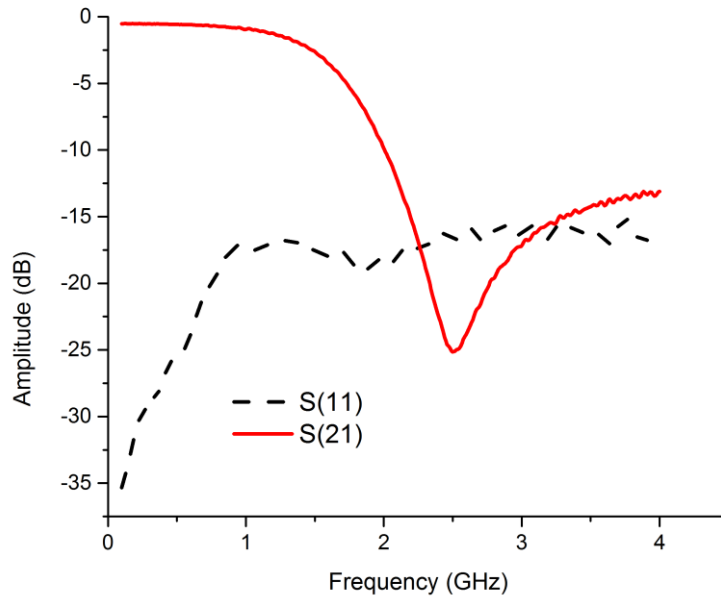


Figure 3.24. Measured result of the low-pass filter from Mini-circuits.

3.2.8 17.5-18 GHz Wilkinson power divider design

Wilkinson power divider was invented by E. J Wilkinson [14]. The most simple structure of Wilkinson power divider is a three-port passive circuit that is able to divide input power from port 1 into two equal portions between ports 2 and port 3 whereas all three ports are matched. The most important traits of Wilkinson power divider is the high isolation between output port 2 and port 3. The simpler structure of Wilkinson power divider is shown in Figure 3.25. It consists of two quarter-wavelength branches and one resistor connecting the two output ports. The main problem of this structure is related to its narrow bandwidth. Some techniques have been used for improving the bandwidth of Wilkinson power divider such as [26] [27] [28].

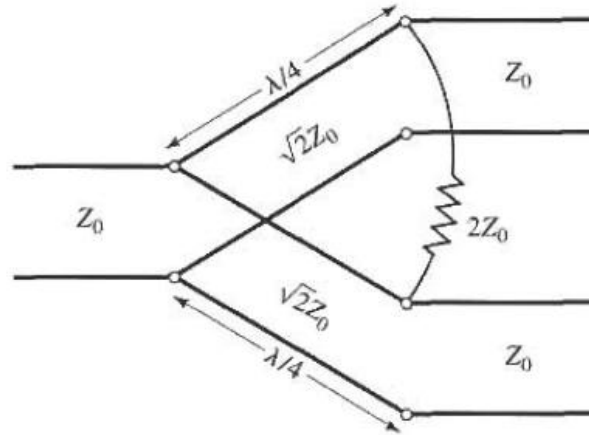


Figure 3.25. The structure of Wilkinson power divider [12].

For the Wilkinson power divider design, several problems arise when the working frequency is above X-band (8-12 GHz). First of all, at such high frequency the size of the power divider should be very small, which means that the two branches of the power divider are very close to each other. A strong coupling between the two branches could destroy the split power ratio of the divider. Secondly, wide low-impedance lines at the higher frequencies make it impossible to bend the branches in a semi-circle [29]. In order to solve these problems [29], a new structure of power divider is proposed, where 270° rather than 90° transmission line is used for the two branches. 100 ohms resistor is placed between the two 180° 50 ohms lines. The structure of the designed Wilkinson power divider is shown in Figure 3.26.

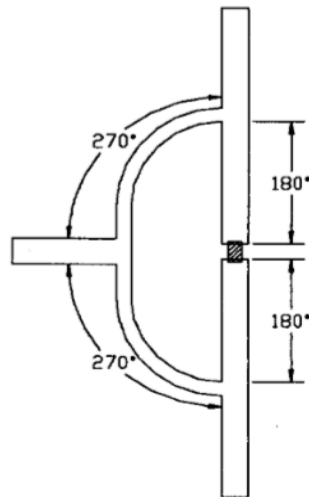


Figure 3.26. Proposed structure of Wilkinson power divider in [29].

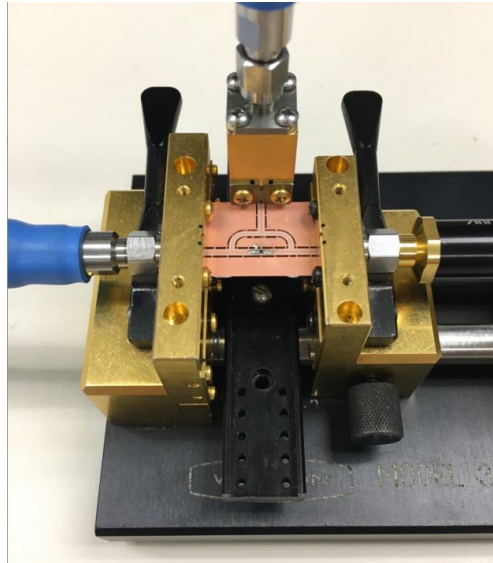


Figure 3.27. Fabricated 17.5-18 GHz Wilkinson power divider.

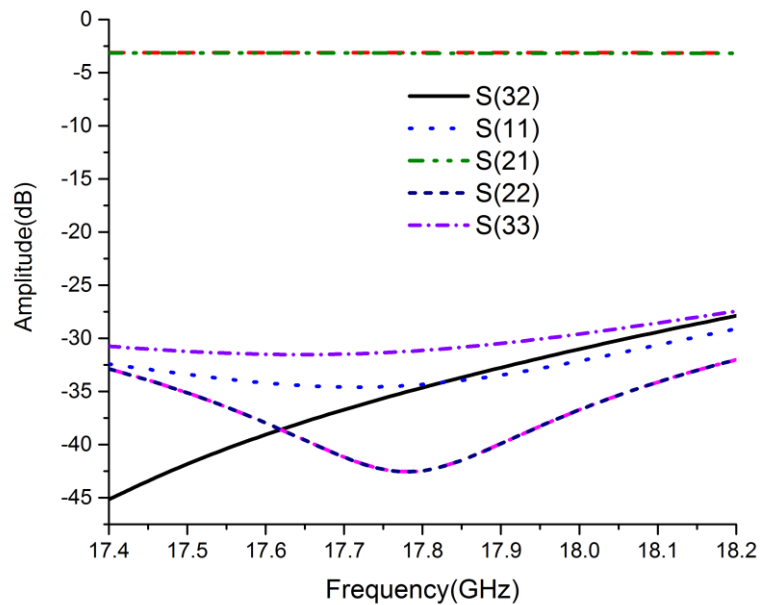


Figure 3.28. Simulated results of our Wilkinson power divider.

Simulated result is shown in Figure 3. 28. The insertion loss S(21) and S(31) are -3.1 dB from 17.5 GHz to 18 GHz. The return loss at each port S(11), S(22) and S(33) are all under -30 dB. The isolation between the two output ports S(23) is also under 30 dB from 17.5 to 18 GHz.

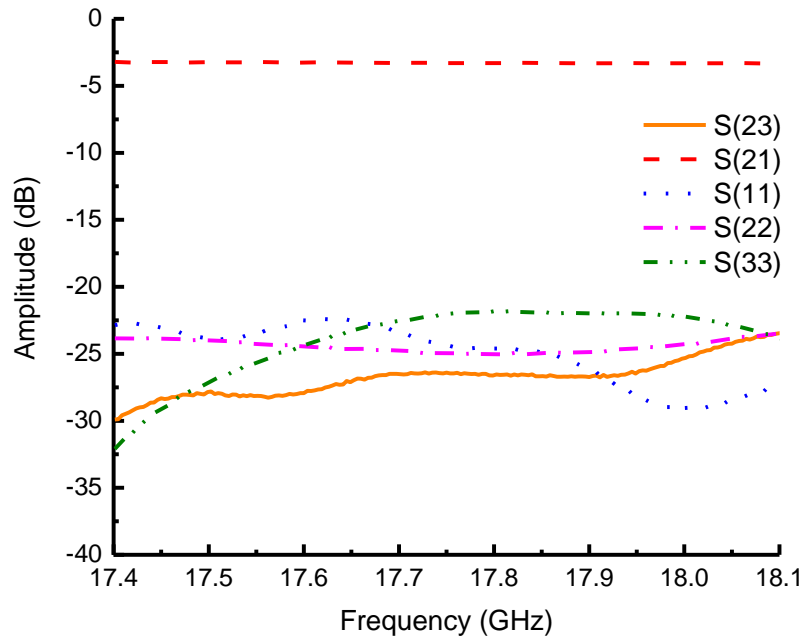


Figure 3.29. Measured results of our Wilkinson power divider.

Measured results in Figure 3.29 show that the insertion loss from port 1 to port2 and from port 1 to port 3 are -4 dB over the bandwidth. All three ports are well matched because the return loss at each port is well under -20 dB. The isolation between port 2 and port 3 is under -25 dB.

3.2.9 Two SIW filters design

In recent years, a large number of passive circuits using SIW technology have been proposed and designed such as SIW filters, SIW couplers, SIW power dividers, circulators and antennas.

In these passive SIW circuits, filters have received a particular attention. The disadvantages of conventional waveguide filters including high cost, heavy weight and difficulty to fabricate. Conventional planar filters such as microstrip filters and strip-line filters are hard to fabricate when frequency goes into the millimeter wave range. SIW technique paves the way to fabricate filters with ordinary PCB process. So the fabricated SIW filter is low cost, light weight, small size, easy to integrate with other planar circuit and it does not need tuning [30]. Various filter topologies have been proposed. Figure 3.30 shows 4 typical topologies of SIW filter design.

In this reader design, based on the design theory in, two SIW filters are designed [30] in order to suppress the undesired signal at the output of mixer and the output of multiplier. The passband of the two SIW filters are 17.5GHz-18GHz and 35-36GHz, respectively.

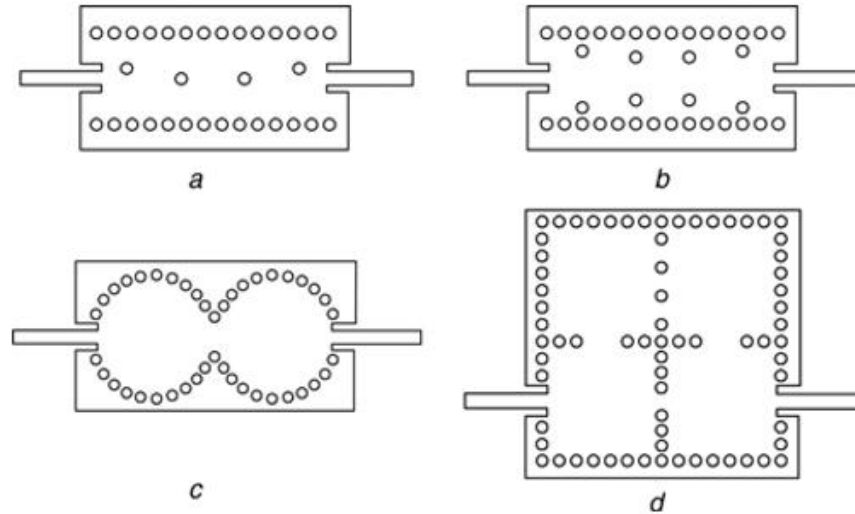


Figure 3.30. Different types of SIW filters. (a) Filter with inductive-post, (b) Filter with iris windows, (c) Filter with circular cavities, (d) Filter with rectangular cavities and cross-coupling. [19].

First of all, for the 17.5-18GHz band-pass filter design, the dimensions of filter are shown in Figure 3.31 and Table 3.8. Figure 3.32 shows the comparison between the simulated and measured results. The measured results show that the insertion loss in pass-band is -3.5 dB. Return loss are all under -20 dB in the pass-band in both simulated and measured results.

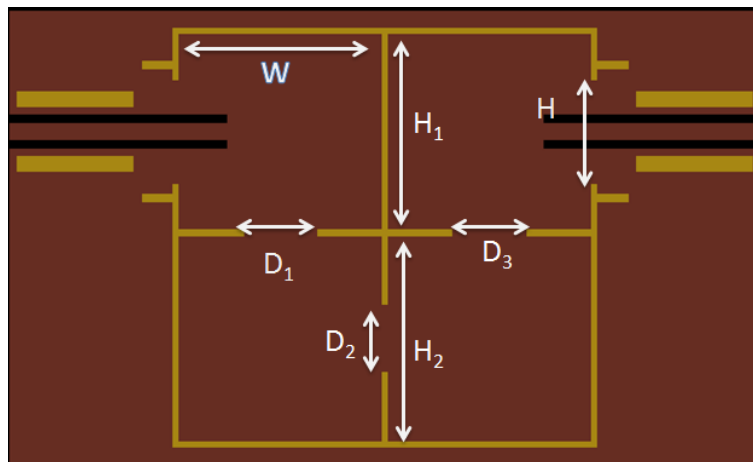


Figure 3.31. Layout of the designed 17.5-18 GHz SIW filter.

Table 3.7. Dimensions of the designed 17.5-18 GHz SIW filter.

Size	Value (mil)	Size	Value (mil)
W	260.2	D1	94.4
H	312.8	D2	86.6
H1	250.8	D3	94.4
H2	262.2		

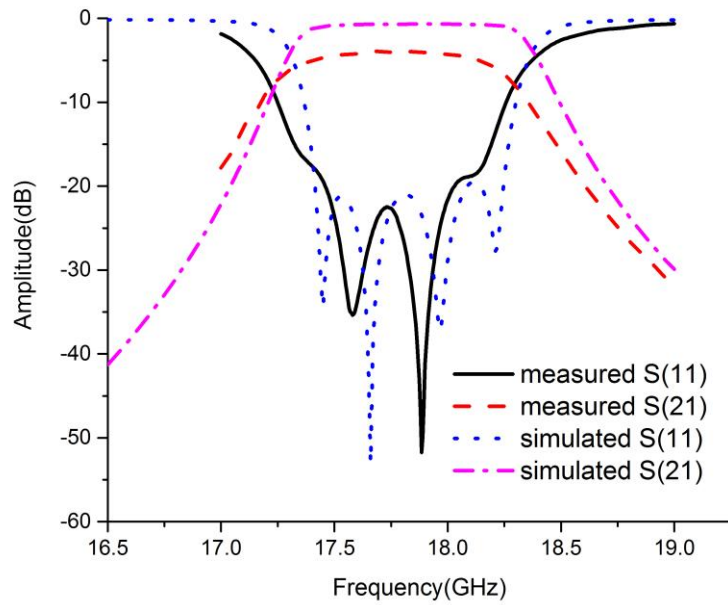


Figure 3.32. Measured and simulated results of the 17.5-18 GHz SIW filter.

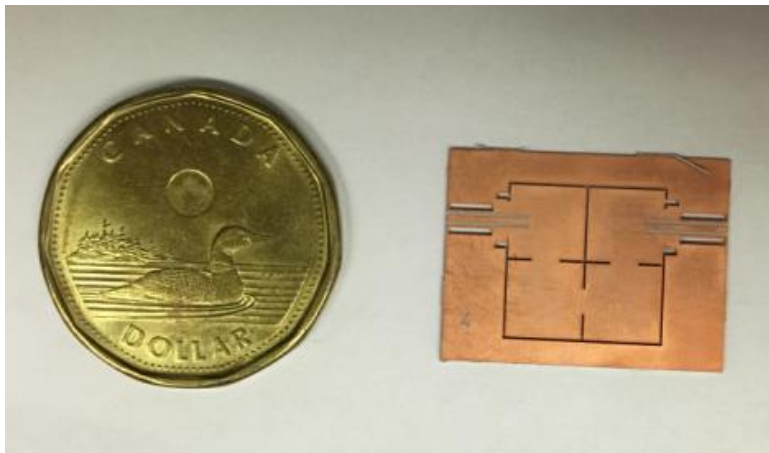


Figure 3.33. Fabricated 17.5-18 GHz SIW filter.

The 35-36 GHz 4 cavities SIW filter is also designed. The dimensions of the filter are shown in Figure 3.34. Both the simulated and measured results are shown in Figure 3.35. According to Figure 3.34, the pass-band return loss in the test result is under -15 dB which is acceptable. The insertion loss of the test result in connection with the pass band is nearly -3 dB. Table 3.9 shows the size of the designed filter.

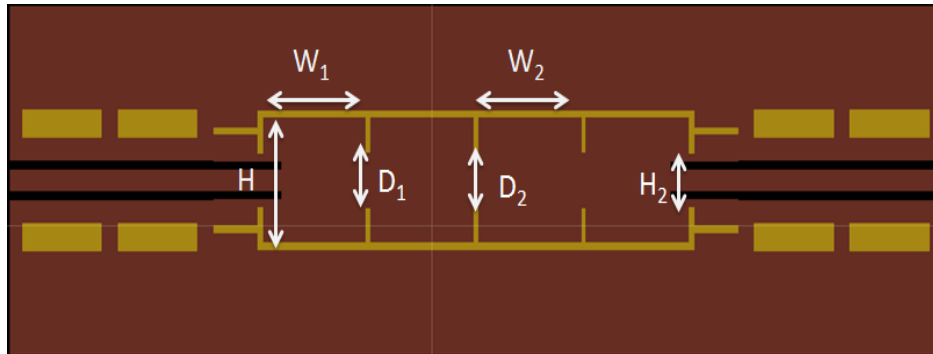


Figure 3.34. Layout of the designed 36-36 GHz SIW filter.

Table 3.8. Dimensions of the designed 36-36 GHz SIW filter.

Size	Value (mil)	Size	Value (mil)
W1	129	W2	129.6
H	132	D1	55.6
H2	55.8	D2	59.6

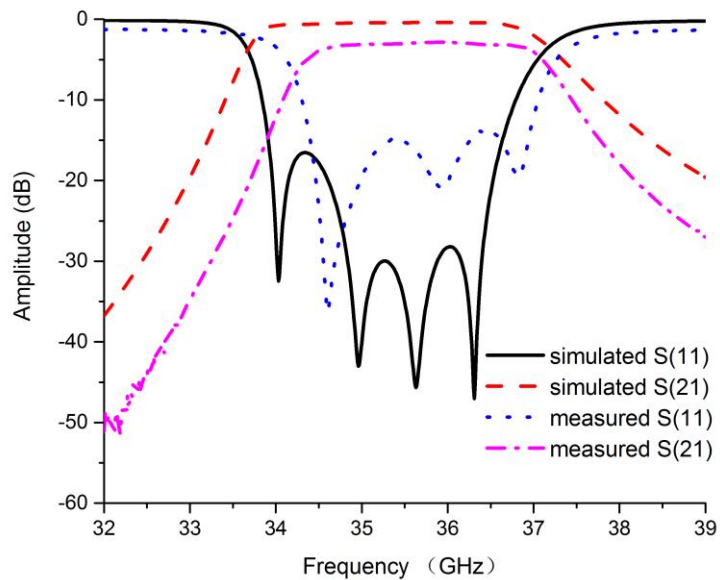


Figure 3.35. Simulated and measured results of our 35-36 GHz SIW filter.

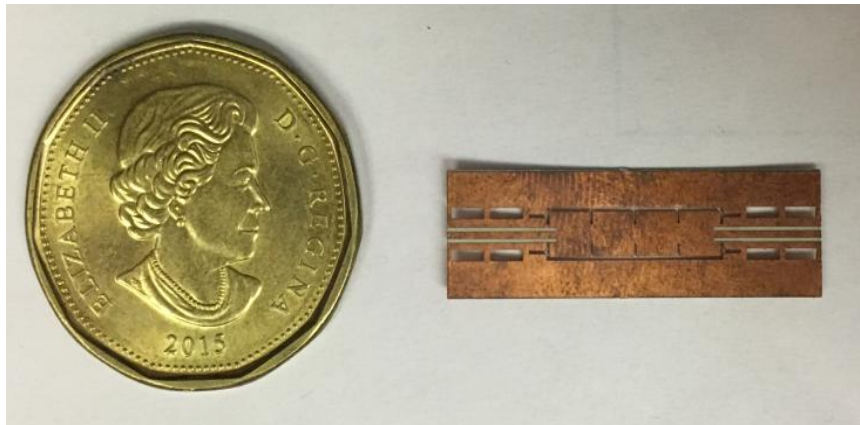


Figure 3.36. Fabricated 35-36 GHz four SIW cavities filter.

3.2.10 HMC579 (Multiplier)

HMC 579 is a X2 active broadband frequency multiplier. The input frequency range is 16-23GHz and the output frequency range is from 32 GHz to 46 GHz. HMC 579 is a die which means there is no any package on it. So a wire-bonding technique is needed to mount the die on our PCB board. Using the wire bonding technique in the Poly-Grames Research Center, the input and output of chip can be connected to the PCB board, so the chip could work well as a part in the whole system.

On the PCB board, a small rectangle slot should be reserved to place the die and a bypass capacitor. The gap between the die and the transmission line should be made as close as possible and a normal distance between chip and transmission is 3 mil.

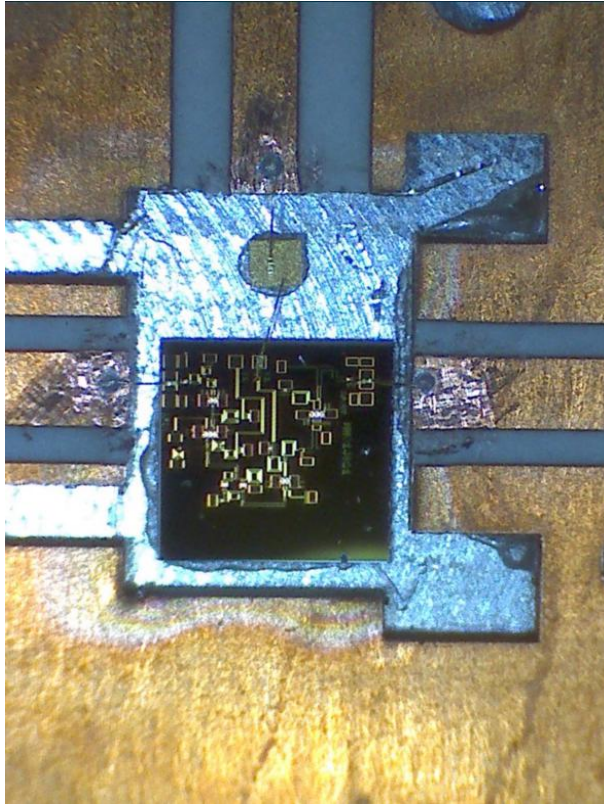


Figure 3.37. Wire-bonding technique under our microscope.

3.2.11 LC bandpass filter design

In the receiver of our reader, a LC band-pass filter is designed to suppress the spurious signal of output signal from the sub-harmonic mixer. The band-pass filter is designed in ADS, simulation is shown in Figure3.39. The passband of this filter is 2 MHz-5 MHz.

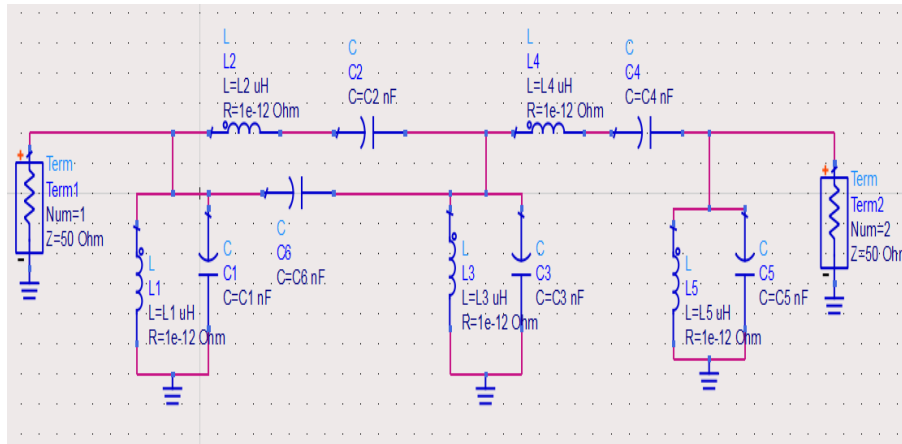


Figure 3.38. Schematic diagram of the LC bandpass filter.

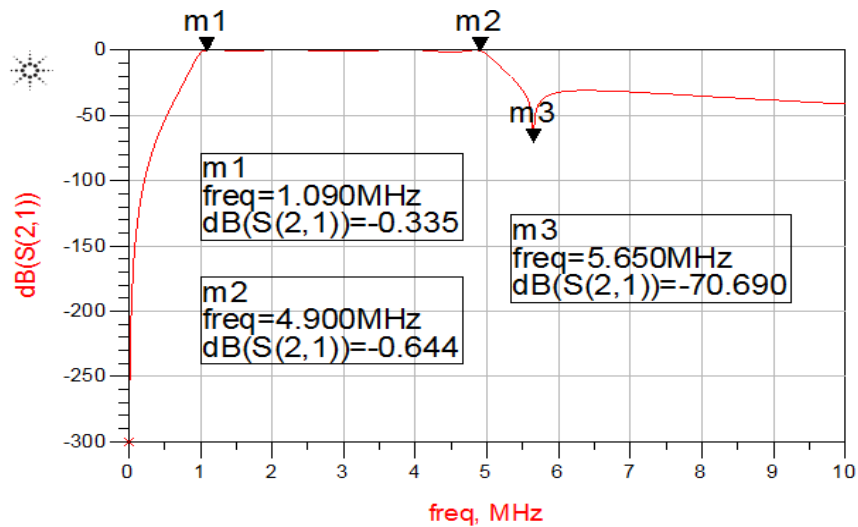


Figure 3.39. Measured result of the LC bandpass filter.

3.2.12 VGA (variable gain amplifier) module design

In RF and microwave systems, VGA is normally placed at the IF stage of the receiver. In this VGA design, we use AD 8338 as the required VGA chip. The voltage controlled gain range of AD 8338 chip is from 0 dB to 80 dB. The working frequency is up to 18 MHz. Because the AD8338 input is a fully differential signal path, a differential-to-single-ended amplifier is needed before the chip. On the other hand, because the output of AD8338 is also differential path, a single-to-differential-ended amplifier AD8131 is also needed at the output of AD 8338. The LC bandpass filter and the VGA circuits are integrated in one PCB board. PCB substrate is FR4. Figure 3.38 shows the circuits structure of the LC bandpass filter and VGA circuits.

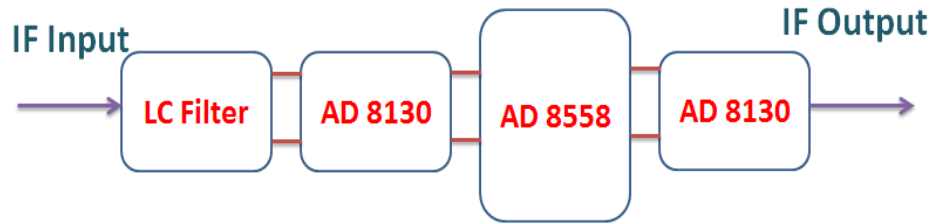


Figure 3.40. Circuits structure of the LC bandpass filter and the VGA circuits.

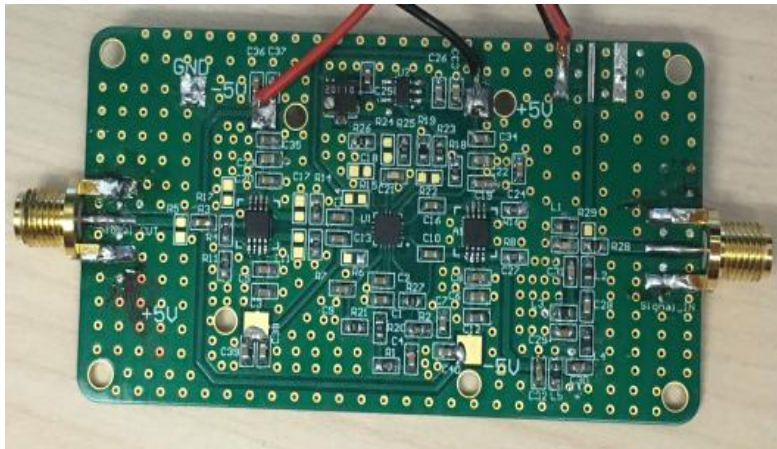


Figure 3.41. Circuit board contains LC filter and VGA circuits.

Measured results show that when input is -50 dBm, controlled voltage is 0.75 V, The output of the VGA circuits is more than 2 dB and gain of the VGA circuits is at least 47 dB. Figure 3.43 shows the output of our VGA circuits in the passband (from 1 MHz to 6 MHz). Figure 3.42, Figure 3.43 and Figure 3.44 show the output power at 1.5 MHz, 3 MHz and 4 MHz, respectively.

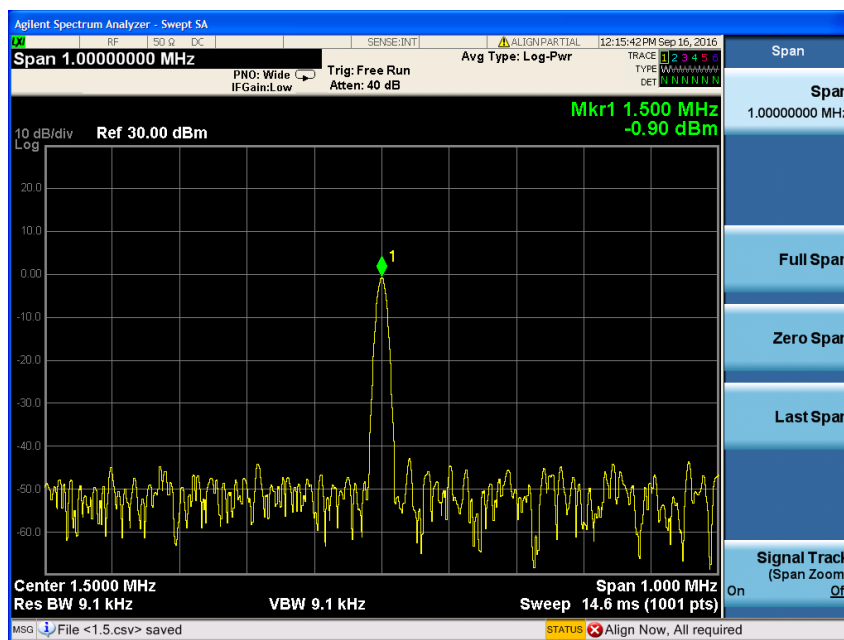


Figure 3.42. Output power at 1.5 MHz.

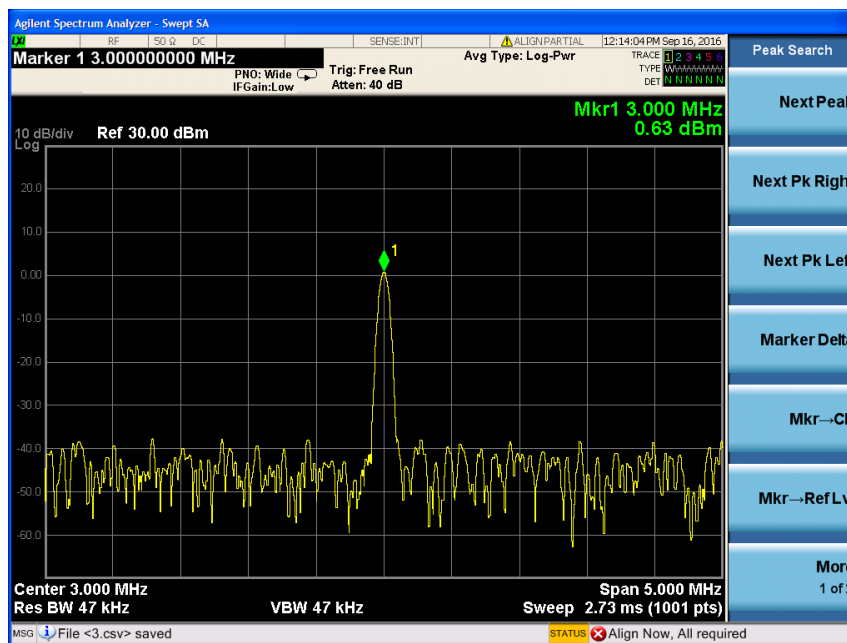


Figure 3.43. Output power at 3 MHz.

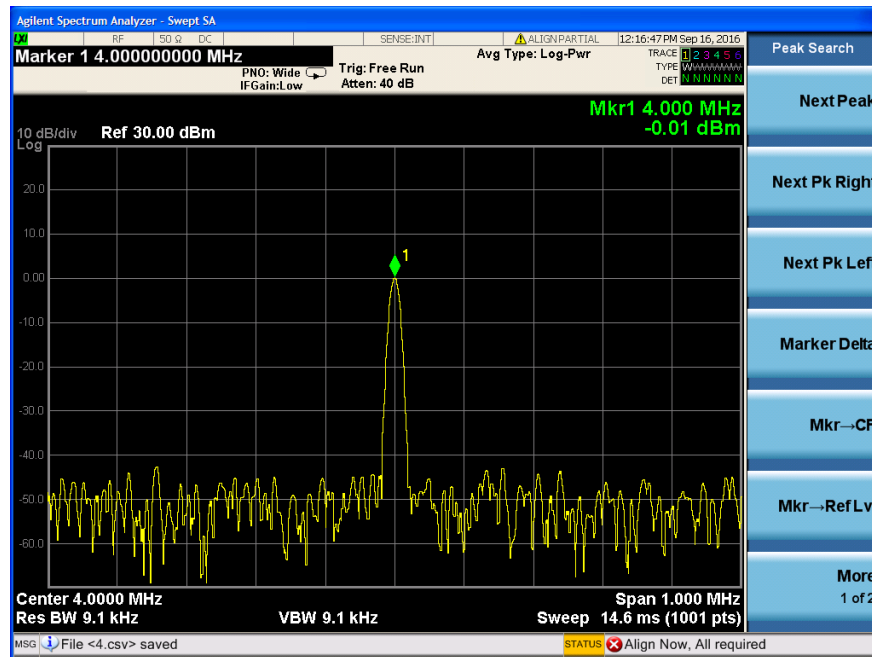


Figure 3.44. Output signal at 4MHz.

CHAPTER 4 SYSTEM MEASUREMENT

4.1 Transmitter Measurement

After designing and testing all the above-described passive circuits, the system board was fabricated. Since most circuits are related to the transmitter, it was necessary to test the transmitter. The fabricated transmitter board is shown in Figure 4.1. In order to prevent the generated signal from radiating into space and also interfering with other signals, a metallic housing was also fabricated. Figure 4.2 shows the one tone signal of transmitted power. The phase noise of this one tone signal is shown in Figure 4.3.

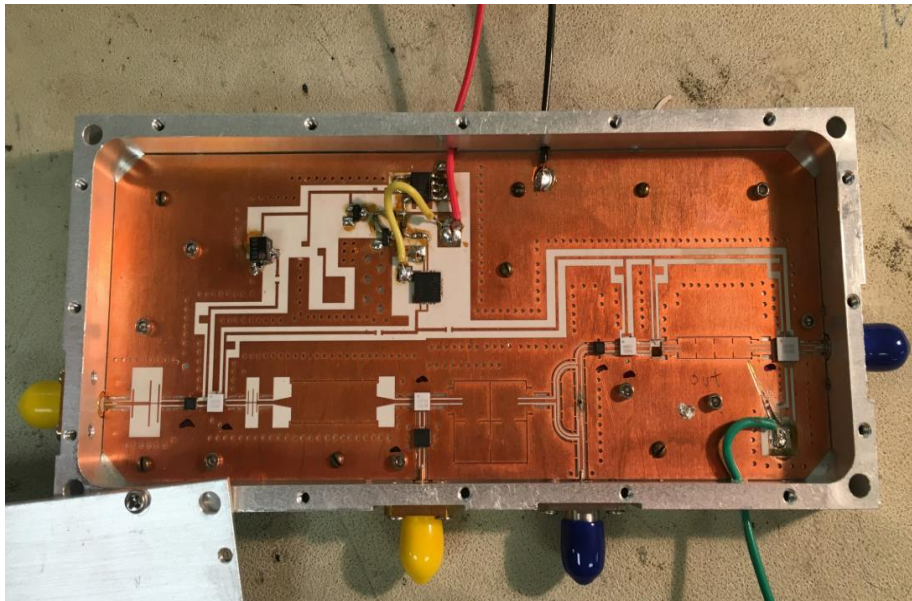


Figure 4.1. Fabricated transmitter of our reader system.

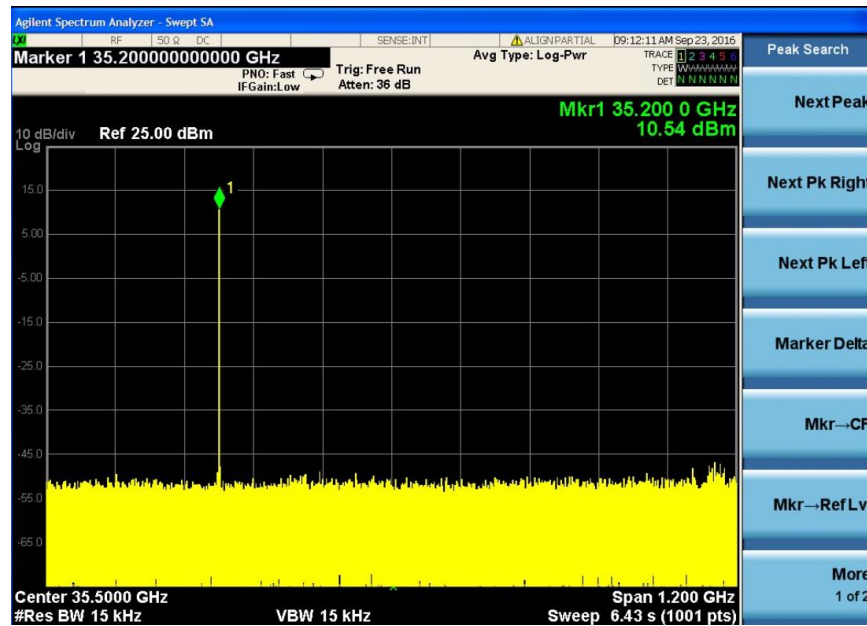


Figure 4.2. Phase noise of one tone signal.

When DDS generates output frequency at 1GHz, the LO signal of PLL is 8.3 GHz, the transmitted power is at 35.2 GHz, after considering cable loss, the total output power should be 22 dBm.



Figure 4.3. Output signal of our transmitter.

In Figure 4.3, the output signal power level from 35 to 36 GHz is not the same. This situation is caused by the multiplier. Even the input power are the same, the output power at different frequencies are not at the same power level.

4.2 Measurements of the transceiver system

In a transceiver system design, due to the fact that there are more than one active circuit, the issue of power supply is another important aspect in the system design. In order to make the system compact and simplify the test procedure, a power supply board is designed. Table 4.1 shows all the active circuits in the reader. Figure 4.4 shows the power supply board of the reader.

Table. 4.1. Active circuits and their DC supplies of reader.

Component	Power Supplies	Component	Power Supplies
HMC 573	Vdd=5 V	HMC 579	Vdd= 5 V
	Vgg=-1.5 V	HMC 1040	Vdd=2.5 V
HMC451	Vdd=5 V	HMC 339	Vdd= 4 V
HMC 635	Vdd= 5 V		
	Vgg=- 0.8 V		

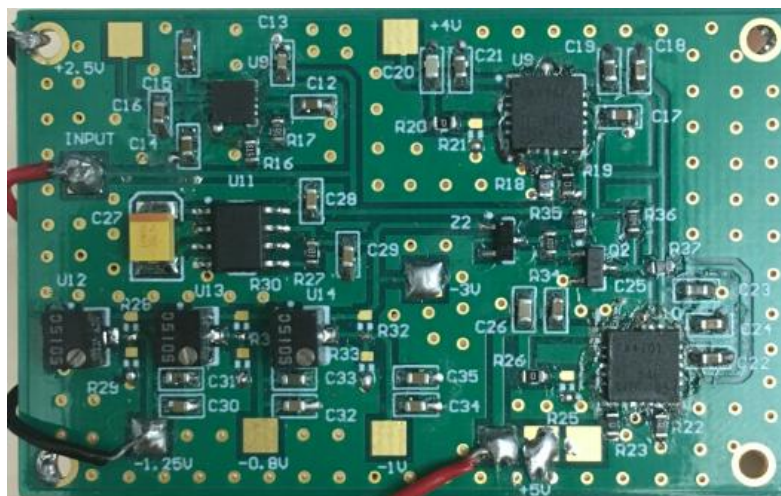
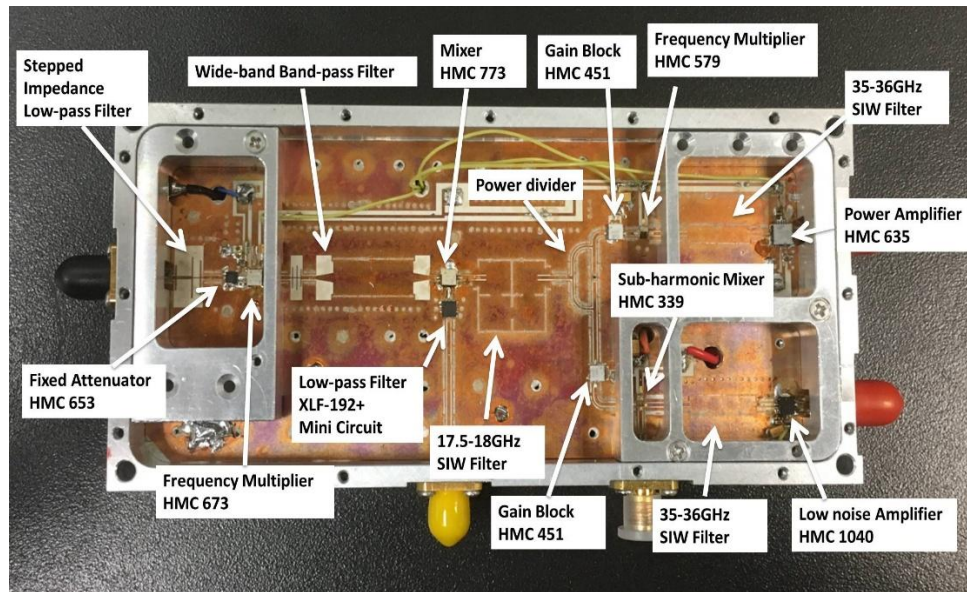
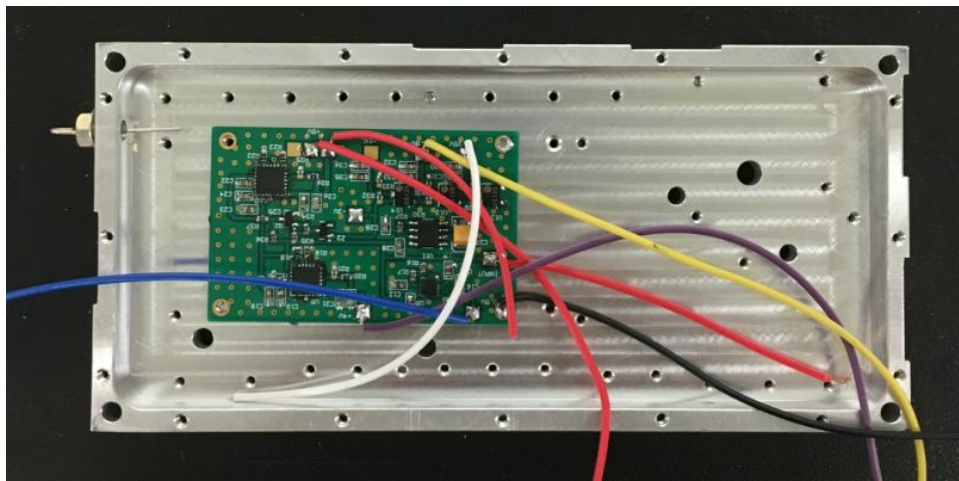


Figure 4.4. Fabricated power supply board.



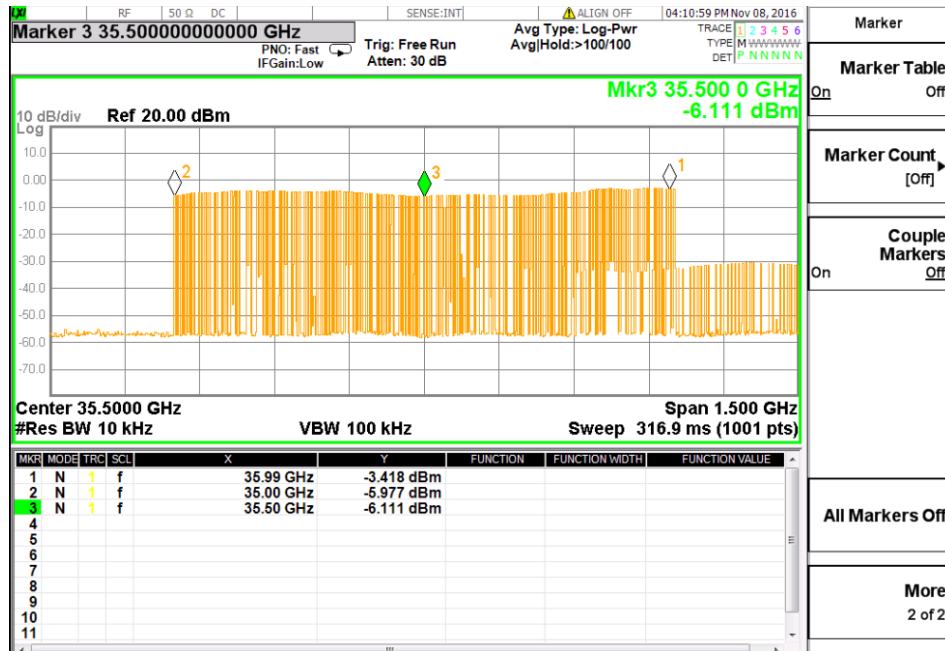
(a)



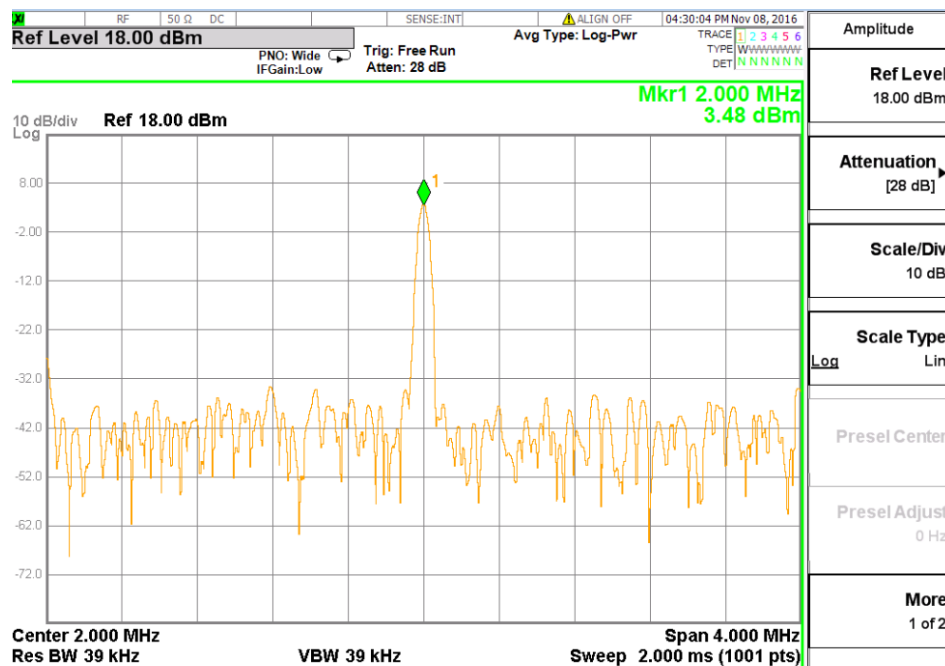
(b)

Figure 4.5. Fabricated reader system with a metallic housing.

The metallic housing of the transceiver consists of two floors. The front floor is placed on the transceiver board. The second floor in the back is placed on the power supplies board. The voltage powers are supplied through a wire that goes through the metallic housing. Since there is no frequency domain chipless tag at this frequency in the laboratory, the way to measure the transceiver is to generate a signal to replace the actual signal from the tag. In order to verify the transceiver, the output power of signal generator is -50 dBm, the frequency range of the signal generator is set from 35.002GHz - 36.002 GHz, corresponding to a bandwidth of 1GHz .



(a)



(b)

Figure 4.6. Measured results of the transceiver (a) transmitted signal, (b) output at 4 MHz.

In the transmitter side, the actual transmitted signal power is 21 dBm which well matches with the test result of the single transmitter module.

In the receiver side, the LO signal is the output signal of the power divider in the transmitter, RF signal is the signal generated from the signal generator. After down-converting of sub-harmonic mixer HMC 339, and amplified by VGA, the IF signal at 2MHz is shown through a frequency analyzer. The output power is 3.48dBm.

Comparing measured results with simulated results in chapter 3, the measured results of the transmitted power and received power are well matched with the simulated results.

CONCLUSION AND FUTURE WORK

The reader design for chipless MMID tag is presented and validated in this dissertation. Chipless tag means the tag is fully passive and there is no IC (integrated circuit) on it. The information or code is encoded in the frequency domain. This designed reader can be used to communicate with the chipless tag. On the other hand, the working frequency of this identification system is over the millimeter-wave frequency range. For our reader design, the interrogation signal of reader is FMCW (frequency-modulated continuous-wave) signal. As the tag receives this interrogation signal, a frequency signature would appear in the frequency domain. The reader finally receives the signal with the information of the tag. The working distance of this system is designed for operation from 3 to 10 meters. The whole reader including transmitter and receiver is finally designed and tested. Before the reader is demonstrated, three basic issues are thoroughly discussed and analyzed. All of them make it possible to design and validate the reader system.

1) Discussion of the three methods generating FMCW interrogation signal

All the three methods are discussed in this thesis. PLL, DDS and VCO are used in these three methods. FMCW signal could be directly generated either by DDS or VCO. The method that makes use of a mixer to mix up the output signal of DDS and PLL is adopted due to its simple structure and high output quality.

2) Discussion about the three reader topologies

After discussing the three methods to generate interrogation signal, the reader topology is also examined in this thesis. According to the specifications of our reader design considerations such as realizability issues, cost issue and simple level of the system, the three topologies are compared.

3) Passive circuits design

In this reader design, the passive circuits including a low-pass filter, three band-pass filters and a power divider are designed. SIW technology is used to design the band-pass filters. Stepped-impedance low-pass filter is presented thanks to its simple structure and small size. Another band-pass filter is designed by combining a low-pass filter and an SIW transmission line together. These passive circuits have all achieved good simulated and measured results.

The final system board is fabricated and tested. The test results show that the transmitted FMCW signal is 35-36 GHz and power level is at 22 dBm. The receiver part of our reader is tested by sending to the receiver a difference signal of the interrogation signal.

When looking back of the thesis work, the research contributions presented in this thesis may be extended as part of future work in the following ways.

1) MMID system test

Because there is no chipless tag which is working at 35-36 GHz right now, the fabricated reader is not able to communicate with the tag. In the future, as long as the specific tag is designed and tested, a functional MMID system could be implemented through the use of the presented reader system.

2) Testing principle of chipless tag

In the DDS module, two parameters (time step and frequency step) determine the sweeping speed of DDS. So in theoretical analysis and practical operation, how these two parameters would affect the measured results of identifying a tag if changing frequency step and time step in DDS. This is a crucial issue to consider because these varying parameters are related to the signal processing in connection with the received signal from the reader.

BIBLIOGRAPHY

- [1] S. Preradovic, I. Balbin, N. C. Karmakar, and G. F. Swiegers, "Multiresonator-Based Chipless RFID System for Low-Cost Item Tracking," *IEEE Transactions on Microwave Theory and Techniques*, vol. 57, pp. 1411-1419, 2009.
- [2] S. A. Ahson and M. Ilyas, *RFID handbook: applications, technology, security, and privacy*: CRC press, 2008.
- [3] N. C. Karmakar, R. Koswatta, P. Kalansuriya, and E. Rubayet, *Chipless RFID reader architecture*: Artech House, 2013.
- [4] D. M. Dobkin, *The rf in RFID: uhf RFID in practice*: Newnes, 2012.
- [5] S. Preradovic and N. Karmakar, "Chipless millimeter wave identification (MMID) tag at 30 GHz," in *Microwave Conference (EuMC), 2011 41st European*, 2011, pp. 123-126.
- [6] P. Pursula, T. Vaha-Heikkila, A. Muller, D. Neculoiu, G. Konstantinidis, A. Oja, et al., "Millimeter-Wave Identification; A New Short-Range Radio System for Low-Power High Data-Rate Applications," *IEEE Transactions on Microwave Theory and Techniques*, vol. 56, pp. 2221-2228, 2008.
- [7] O. Necibi, S. Beldi, and A. Gharsallah, "Design of a chipless RFID tag using cascaded and parallel spiral resonators at 30 GHz," in *Web Applications and Networking (WSWAN), 2015 2nd World Symposium on*, 2015, pp. 1-5.
- [8] C. A. Balanis, *Antenna theory: analysis and design*: John Wiley & Sons, 2016.
- [9] W. L. Stutzman and G. A. Thiele, *Antenna theory and design*: John Wiley & Sons, 2012.
- [10] K. Chang, *RF and microwave wireless systems vol. 161*: John Wiley & Sons, 2004.
- [11] I. Hunter, *Theory and design of microwave filters*: Iet, 2001.
- [12] D. M. Pozar, *Microwave engineering*: John Wiley & Sons, 2009.
- [13] G. R. Branner, B. P. Kumar, and D. G. Thomas, "Design of microstrip T junction power divider circuits for enhanced performance," in *Circuits and Systems, 1995., Proceedings., Proceedings of the 38th Midwest Symposium on*, 1995, pp. 1213-1215 vol.2.

- [14] E. J. Wilkinson, "An N-Way Hybrid Power Divider," IRE Transactions on Microwave Theory and Techniques, vol. 8, pp. 116-118, 1960.
- [15] J. Detlefsen, A. Dallinger, S. Schelkshorn, and S. Bertl, "UWB Millimeter-Wave FMCW Radar using Hubert Transform Methods," in 2006 IEEE Ninth International Symposium on Spread Spectrum Techniques and Applications, 2006, pp. 46-48.
- [16] L. Tian, X. Zhu, Y. Li, L. Yang, and P. Miao, "Investigation of wideband synthesizer covering 16GHz to 32GHz," in 2013 6th UK, Europe, China Millimeter Waves and THz Technology Workshop (UCMMT), 2013.
- [17] T. Djerafi, K. Wu, A. Marque, and A. Ghiotto, "Chipless substrate integrated waveguide tag for millimeter wave identification," in Millimeter Waves (GSMM), 2015 Global Symposium On, 2015, pp. 1-3.
- [18] F. He, "Innovative Microwave and Millimetre-Wave Components and Sub-Systems Based on Substrate Integration Technology," École Polytechnique de Montréal, 2011.
- [19] M. Bozzi, A. Georgiadis, and K. Wu, "Review of substrate-integrated waveguide circuits and antennas," IET Microwaves, Antennas & Propagation, vol. 5, pp. 909-920, 2011.
- [20] X. P. Chen and K. Wu, "Substrate Integrated Waveguide Cross-Coupled Filter With Negative Coupling Structure," IEEE Transactions on Microwave Theory and Techniques, vol. 56, pp. 142-149, 2008.
- [21] C. Ji-Xin, H. Wei, H. Zhang-Cheng, L. Hao, and W. Ke, "Development of a low cost microwave mixer using a broad-band substrate integrated waveguide (SIW) coupler," IEEE Microwave and Wireless Components Letters, vol. 16, pp. 84-86, 2006.
- [22] Y. Cassivi and K. Wu, "Low cost microwave oscillator using substrate integrated waveguide cavity," IEEE Microwave and Wireless Components Letters, vol. 13, pp. 48-50, 2003.
- [23] M. Abdolhamidi and M. Shahabadi, "X-Band Substrate Integrated Waveguide Amplifier," IEEE Microwave and Wireless Components Letters, vol. 18, pp. 815-817, 2008.
- [24] Y. Li, H. Wei, H. Guang, C. Jixin, W. Ke, and C. Tie Jun, "Simulation and experiment on SIW slot array antennas," IEEE Microwave and Wireless Components Letters, vol. 14, pp. 446-448, 2004.

- [25] Z. Zhang, "Substrate Integrated Waveguide Devices and Receiver Systems for Millimeter-Wave Applications," École Polytechnique de Montréal, 2011.
- [26] L. I. Parad and R. L. Moynihan, "Split-Tee Power Divider," IEEE Transactions on Microwave Theory and Techniques, vol. 13, pp. 91-95, 1965.
- [27] R. Pazoki, M. R. G. Fard, and H. G. Fard, "A Modification in the Single-Stage Wilkinson Power Divider to Obtain Wider Bandwidth," in 2007 Asia-Pacific Microwave Conference, 2007, pp. 1-4.
- [28] O. Ahmed and A. R. Sebak, "A modified Wilkinson power divider/combiner for ultrawideband communications," in 2009 IEEE Antennas and Propagation Society International Symposium, 2009, pp. 1-4.
- [29] D. Antsos, R. Crist, and L. Sukamto, "A novel Wilkinson power divider with predictable performance at K and Ka-band," in Microwave Symposium Digest, 1994., IEEE MTT-S International, 1994, pp. 907-910 vol.2.
- [30] Y. Tang, Development of substrate integrated waveguide filters: ProQuest, 2006.